Dissertation for the attainment of
the academic title
doctor rerum naturalium

The cell-type specific role of Amphiregulin in Lupus Nephritis

Presented by
Laura-Isabell Ehnold

Department of Biology
University of Hamburg

1. Reviewer: Prof. Dr. Wolfgang Streit
2. Reviewer: Prof. Dr. Oliver Steinmetz

Hamburg, 20.02.2024

Disputation: 21.06.2024; Reviewer: Prof. Dr. Oliver Steinmetz,
Prof. Dr. Tim Gilberger, Prof. Dr. Tobias Lenz

„Unsere größte Schwäche liegt im Aufgeben. Der sicherste Weg zum Erfolg ist immer, es doch noch mal zu versuchen“

Thomas Alva Edison

The presented work was externally conducted from March 2021 until January 2024 in the III. Department of Medicine at the University Medical Center Hamburg-Eppendorf under the supervision of Prof. Dr. Oliver Steinmetz. Prof. Dr. Wolfgang Streit supervised this work in the Department of Biology at the University of Hamburg

Eidesstattliche Erklärung

Hiermit versichere ich eidesstattlich, dass ich die Arbeit selbständig verfasst und keine anderen als die angegebenen Quellen und Hilfsmittel benutzt habe.

Hamburg, den 20.02.2024

Laura-Isabell Ehnold

Inhaltsverzeichnis

Eidesstattliche Erklärung 4

Inhaltsverzeichnis 5

Acknowledgments 8

I. Index of Tables 9

II. Index of Figures 10

III. Summary 11

IV. Zusammenfassung 12

1. Introduction 13

1.1. Glomerulonephritis 13

1.1.1. Lupus Nephritis 14

1.2. Immune cells in lupus nephritis 15

1.2.1. T helper effector cells in LN 16

1.2.2. Tregs in LN 17

1.2.3. Monocyte/Macrophages 19

1.3. Renal fibrosis 20

1.4. The Amphiregulin/EGFR axis 22

1.5. AREG in Fibrosis 24

2. Material and Methods 27

2.1. Material 27

2.1.1. Equipment 27

2.1.2. Consumables 28

2.1.3. Chemicals 29

2.1.4. Antibodies 29

2.1.5. Kits 32

2.1.6. Cell lines 32

2.1.7. Media and recombinant proteins 32

2.1.8. Buffer and solutions 33
2.1.9. Mice 34
2.1.10. Software and databases 34
2.2. Methods 35
2.2.1. Human glomerular endothelial cells 35
2.2.2. Murine proximal tubules and mesangium cells 35
2.2.3. Scratch-assay 35
2.2.4. Endothelial-tube-formation-assay 36
2.2.5. Animal experiments 36
2.2.6. Leucocyte isolation from tissue 36
2.2.7. Flow cytometry 36
2.2.8. Annexin V-staining 39
2.2.9. Sorting 39
2.2.10. Genomic DNA experiments 39
2.2.11. Murine ELISA analysis 40
2.2.12. Histological staining 41
2.2.13. Periodic acid Schiff staining (PAS) 41
2.2.14. Assessment of renal histological changes 41
2.2.15. Fibrosis staining 42
2.2.16. Immunohistology staining 42
2.2.17. Immunohistology staining of human renal biopsies 42
3. Results 43
3.1. AREG expression is increased in human lupus nephritis 43
3.2. Generation of mice with Treg-restricted deficiency of AREG 45
3.3. Deficiency of AREG in Tregs leads to a worsened renal outcome of pristane-induced LN after 12 months 48
3.4. The absence of AREG derived from Tregs does not affect cellular immune responses 49

3.5. Deficiency of AREG in Tregs does not lead to alterations of macrophage phenotypes 52

3.6. Treg-derived AREG does not alter humoral lupus auto-immunity 53

3.7. Treg-derived AREG ameliorates fibrosis and apoptosis 55

3.8. Macrophage-derived AREG did not alter the renal outcome or fibrosis in pristane-induced LN 57

3.9. The addition of recombinant AREG leads to improved wound healing in vitro. 60

4. Discussion 63

4.1. AREG in human lupus nephritis 64

4.2. Treg restricted AREG knockout 64

4.3. Treg-derived AREG protects from kidney damage in pristane-induced LN 65

4.4. Treg-derived AREG has no impact on T cell responses 66

4.5. No effects of Treg-derived AREG on the macrophage phenotype 66

4.6. AREG from Tregs does not alter humoral lupus immunity 67

4.7. Treg-derived AREG ameliorates kidney fibrosis 67

4.8. Renal tissue protection in LN is a specific feature of Treg-derived AREG 69

4.9. Wound healing effects of AREG 70

4.10. Amphi-Regulin: Discussing the dual regulatory protein 71

4.11. Therapeutic strategies 73

5. Annex 75

5.1. Abbreviation 75

6. References 77

Acknowledgments

I would like to express my deepest gratitude to **Prof. Dr. Oliver Steinmetz** for generously welcoming me into his lab and team. His dedicated guidance, careful review of each data point, and emotional investment in this thesis were invaluable. It was truly a wonderful experience and I appreciate the time spent with you.

A special acknowledgment is reserved for **Prof. Dr. Wolfgang Streit,** who graciously agreed to be my first reviewer. Thank you for this opportunity and for placing your trust in me.

I am immensely thankful to my colleagues who have supported me over the years: Inken Holtze, Dr. Matthias Warkotsch, Dr. Julia Hagenstein, Dr. Simon Melderis, Viona Laas, and Pavels Klimicevs. Our time together during group meetings, visits to the Christmas market, miniature golf and bowling, and pleasant get-togethers over cake, and sparkling wine and crémant were truly enjoyable. Unforgettable is the joy of pizza dinners and rhubarb spritz with Inken, Viona, and Matthias. I would like to thank the clinician who always helped me with the histological analysis.
A big thank you to Renke and Sarah, whose friendship made this experience even more special.

I express my gratitude to my friends and family for standing by me, and a special thanks to my parents. Your steady support has been the driving force behind my journey. I hope to make you proud.

I. Index of Tables

Table 2-1: List of equipment 27
Table 2-2: List of consumables 28
Table 2-3: List of chemicals 29
Table 2-4: List of antibodies for flow cytometry 29
Table 2-5: List of antibodies for histology 31
Table 2-6: List of kits 32
Table 2-7: List of cell lines 32
Table 2-8: List of media and recombinant protein for cell culture 32
Table 2-9: List of buffer and solutions 33
Table 2-10: List of used mice 34
Table 2-11: List of software and databases 34
Table 2-12: Protocol for AREG PCR 40
Table 2-13: Temperature profile 40
Table 2-14: Primer 40
Table 6-1: List of abbreviations used in this study 75

II. Index of Figures

Figure 1: Summary of leucocyte effects in lupus nephritis 16
Figure 2: Overview of AREG-mediated effects 25
Figure 3: Gating strategy for $CD4^+$ Teffs and Tregs 37
Fig.4: Gating strategy for PMN, M1 and M2 macrophages 38
Figure 5. AREG expression is increased in renal infiltrating leukocytes of patients with LN 44
Figure 6: Genetic modification of $AREG^{fl/fl}$ mice 46
Figure 7: Lack of AREG in $FoxP3^{cre}$ x $AREG^{fl/fl}$ mice is limited to Tregs 47
Figure 8: Deficiency of AREG in Tregs aggravates pristane-induced LN 48
Figure 9: The protective effects from Treg-derived AREG are accentuated in the long-term 49
Figure 10: Lack of Treg-derived AREG does not affect CD4+ Teff responses at 12 months of LN 51
Figure 11: Lack of Treg-derived AREG does not affect $CD4^+$ Teff responses at 15 months of LN 52
Figure 12: Lack of AREG in Tregs does not affect macrophage polarization, apoptosis, or proliferation 53
Figure 13: Lack of AREG from Tregs does not affect humoral immune responses 54
Figure 14: Long-term deficiency of AREG from Tregs does not affect humoral immune responses 55
Figure 15: Treg-derived AREG ameliorates renal fibrosis 56
Figure 16: Lack of AREG derived from Tregs leads to increased apoptosis 57
Figure 17: Macrophage-derived AREG does not affect the outcome of LN 58
Figure 18: Lack of AREG in macrophages does not alter renal fibrosis 58
Figure 19: Effects of macrophage-derived AREG on cellular immune responses in LN 59
Figure 20: The addition of recombinant AREG leads to improved wound healing 60
Figure 21: Improved wound healing in human glomerular endothelial cells after the addition of rAREG 61
Figure 22: AREG enhances the growth of renal microvasculature 62

III. Summary

Systemic Lupus erythematosus (SLE) is an autoimmune disease involving multiple organ systems. Lupus nephritis (LN) is one of the most severe manifestations, with high morbidity. We recently identified Amphiregulin (AREG), one of the Ligands of the epidermal-growth-factor-receptor (EGFR), as a potent anti-inflammatory mediator in LN via downregulation of $CD4^+$ T cell activation. In LN AREG is mainly produced by renal infiltrating regulatory T cells (Tregs) and monocytes/macrophages (M/M). Interestingly, studies by us and others have shown, that its function relevantly differs according to the producing cell type. This study therefore aimed to unravel the relevance of cell-type-specific AREG secretion in LN. Conditional knockout mice were used to investigate the role of AREG secreted by $FoxP3^+$ Tregs and $LysM^+$ myeloid cells in the pristane model of chronic LN. In vitro, AREG effects on epithelial tissue regeneration and vascular healing were studied. Mice lacking Treg-derived AREG showed worse LN outcomes with increased glomerular cell proliferation and renal tissue fibrosis. However, cellular, and humoral immune responses remained unaffected. On the other hand, mice with M/M restricted deficiency of AREG secretion showed no change in LN outcome. In vitro, scratch assays of murine mesangial and tubulus cells, as well as human glomerular endothelial cells (hGEnC) showed improved wound healing after incubation with recombinant AREG. In addition, we explored AREG´s effects on the growth and tube formation of hGEnC, which was much facilitated by recombinant AREG. Taken together our data show the important role of Treg-derived AREG for tissue regeneration and protection from detrimental fibrosis in LN.

IV. Zusammenfassung

Der systemische Lupus erythematodes (SLE) ist eine häufige Autoimmunerkrankung, die viele unterschiedliche Organsysteme betreffen kann. Die Lupusnephritis (LN) ist eine der schwersten Manifestationen mit hoher Morbidität. Vor kurzem konnten wir Amphiregulin (AREG), einer der Liganden des epidermalen Wachstumsfaktor-Rezeptors (EGFR), als potenten entzündungshemmenden Mediator der LN identifizieren, der die Aktivierung von pathogenen $CD4^+$ T-Zellen herunterreguliert. Bei der LN wird AREG vor allem von in die Nieren infiltrierenden regulatorischen T-Zellen (Tregs) und Monozyten/Makrophagen (M/M) produziert. Interessanterweise unterscheidet sich seine Funktion je nach dem produzierenden Zelltyp. Ziel dieser Studie war es daher, die Bedeutung der zelltypspezifischen AREG-Sekretion bei der LN zu entschlüsseln. Mit Hilfe von konditionalen Knockout-Mäusen wurde die Rolle von AREG, das von $FoxP3^+$ Tregs und $LysM^+$ myeloischen Zellen sezerniert wird, im Pristane-Modell der chronischen LN untersucht. In vitro wurden die Auswirkungen von AREG auf die Regeneration von Epithelgewebe und die Gefäßheilung untersucht. Mäuse, denen AREG aus Tregs fehlte, zeigten einen schlechteren Verlauf der LN mit erhöhter glomerulärer Zellproliferation und Fibrose des Nierengewebes. Die zellulären und humoralen Immunantworten blieben jedoch unbeeinflusst. Bei Mäusen mit einem M/M-spezifischen Mangel an AREG-Sekretion zeigte sich dagegen keine Veränderung des Verlaufes der LN. In vitro zeigten Scratch-assays an mesangialen und tubulären Zellen der Maus sowie an menschlichen glomerulären Endothelzellen (hGEnC) eine verbesserte Wundheilung nach Inkubation mit rekombinantem AREG. Darüber hinaus untersuchte ich die Auswirkungen von AREG auf das Wachstum und die Formation tubulärer Strukturen von hGEnC, welche durch rekombinantes AREG erheblich gefördert wurden. Insgesamt zeigen meine Daten die wichtige Rolle von Treg-sezerniertem AREG für die Geweberegeneration und den Schutz vor schädlicher Fibrose bei der LN.

1. Introduction

1.1. Glomerulonephritis

Immunologically mediated inflammation of the renal glomeruli is called glomerulonephritis (GN). GN is a major cause of loss of kidney function. The importance of a functional kidney is not deniable; it filters the blood and removes toxic and metabolic substances as well as waste products. Even more, they are necessary for reabsorbing nutrients, maintaining the electrolyte and water household, and with this, regulating blood pressure. The glomeruli are part of the nephron, which is a functional unit in the kidney. Glomeruli consist of a capillary tuft with a complex filtration barrier, which is surrounded by the urinary space, and the Bowman's capsule, which is lined by epithelial cells. The multilayered filtration barrier consists of specialized vascular endothelial cells, which are attached to the glomerular basement membrane (GBM). The final layer of the filtration barrier outside of the GBM is formed by highly specialized epithelial cells, called podocytes, and their delicate foot processes. The capillary tuft is supported by the so-called mesangium, which consists of mesangial cells and extracellular matrix. Our blood is filtered in the glomeruli, which results in the primary urine consisting of water, minerals, and soluble toxins. This primary urine is afterward concentrated by reabsorption processes in the renal tubuli, consisting of the functionally different proximal tubules, the loop of Henle, and the distal tubule segments. The interstitium between the tubules is colonized by fibroblasts as well as leukocytes including dendritic cells (DCs), macrophages, and T cells. If inflammation in the form of GN leads to the destruction of the glomeruli, the filter function of the kidney is severely impaired [1]–[5]. In some types of GN, vascular necrosis develops, the filtration barrier is destroyed, and pro-inflammatory cytokines and chemokines are released into the Bowman's space. This results in the attraction and extravasation of leukocytes, the proliferation of the epithelial cells lining the Bowman's capsule, and finally in the formation of so-called glomerular crescents [6], [7]. Together with a severe decline in renal function, this form of GN is called a rapidly progressive GN (RPGN) and is the most severe form of GN. It can lead to end-stage renal disease within days or weeks. RPGN is characterized by its histo-pathological findings into three different

groups. The first one is the anti-neutrophil cytoplasmatic antibody (ANCA)-associated GN, also named pauci-immune GN, where only sparse depositions of immune complexes can be detected. The second form is the anti-glomerular basement membrane (anti-GBM) GN. In this form, autoantibodies against the renal basal membrane are produced and deposited along the membrane. The third subtype of crescentic GN is the immune-complex mediated form. A typical pathology resulting in this type of RPGN is systemic lupus erythematosus (SLE) with its characteristic renal involvement called lupus nephritis (LN) [6], [8].

1.1.1. Lupus Nephritis

LN is one of the most severe manifestations of SLE. SLE is an auto-immunologically mediated disease in which a high percentage of patients develop LN within 5 years of diagnosis [9]–[11]. Despite decades of intensive research, LN remains a major cause of morbidity and mortality within the SLE cohort [10], [12], [13]. Currently, available treatment options for LN often fail to induce disease remission and are limited by severe side effects such as toxicity, infections, and malignancies. As a result, roughly 10% of patients with LN develop end-stage-kidney disease (ESKD) within 10 years. Therefore, a more effective and targeted treatment of LN is highly warranted [14]–[16]. In order to develop novel treatment strategies, a profound understanding of LN pathophysiology is required. One primary immunological hallmark of SLE and lupus nephritis is pathologic type I interferon signaling, mimicking chronic viral infection, which can even be used to measure disease activity in the blood of diseased individuals [17]. Furthermore, cellular apoptosis as well as the clearing of the apoptotic bodies is chronically impaired [18]–[20]. This results in the break of tolerance against mostly nuclear autoantigens and the emergence of antibodies against anti-double-stranded DNA and other nuclear components [21]–[26]. Multiple cells of the immune system are consequently activated and dysregulated, including both the humoral as well as cellular axes of the adaptive and innate immune systems.

1.2. Immune cells in lupus nephritis

Pathogenic mechanisms in LN originate from an inflammatory response triggered by immunogenic endogenous nuclear antigens e.g., chromatin and histone components. This material activates DNA and RNA sensors such as Toll-like-receptor 7 (TLR7). This activation occurs predominantly within innate immune cells and B cells, subsequently leading to increased cellular activation as well as enhanced levels of type I interferon and various pro-inflammatory cytokines [26].

Importantly, this immune dysregulation culminates in the activation of a broad range of autoreactive T cell subtypes by dendritic cells [26]. Notably, T follicular helper cells (TfH) stimulate germinal center B cells to generate nephritogenic autoantibodies, T helper 1 cells (Th1) contribute by producing macrophage activating Interferon-gamma (IFNγ), and Interleukin 17 (IL-17)-producing T helper 17 cells (Th17) activate neutrophils which all affect progressive kidney injury [27], [28]. Regulatory T cells (Treg), on the other hand, can suppress B- and T cell activity and therefore provide an effective counterbalance in the fight against autoreactive lymphocytes. The described effects of the different subtypes of the innate and adaptive immune system are summarized in Figure 1.

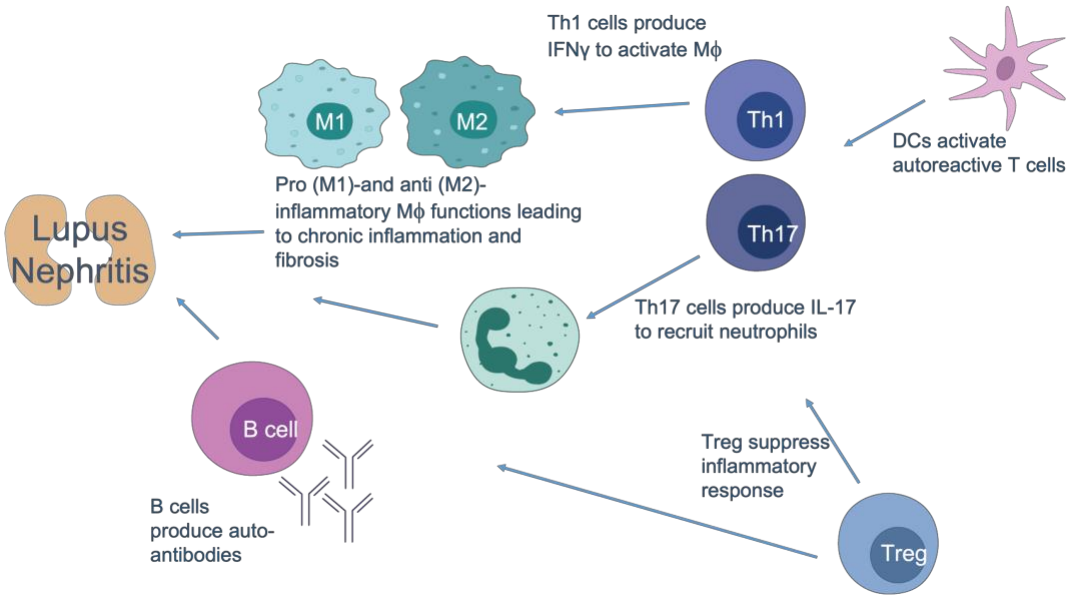

Figure 1: Summary of leucocyte effects in lupus nephritis
Dendritic cells (DCs) which were stimulated by TLR, and type I Interferon signaling present autoantigens and activate autoreactive T cells. T helper 1 cells (Th1) produce pro-inflammatory Interferon-gamma (IFNγ) to activate macrophages (Mϕ), whereas T helper 17 cells produce Interleukin 17 (IL-17) to recruit neutrophils. T cell-mediated activation of pro-inflammatory M1 macrophages and neutrophils, as well as pro-fibrotic M2 macrophages, leads to chronic renal inflammation and fibrosis. T-follicular helper cells (TfH cells) provide help to B cells. Hyperactivity of B cells results in the production of nephritogenic autoantibodies. The inflammatory responses can be suppressed by regulatory T cells (Tregs).

1.2.1. T helper effector cells in LN

T cells can be classified based on their T-cell-receptor (TCR) into γδ-T cells and αβ-T cells. The latter category is subdivided into $CD8^+$ cytotoxic T cells and CD4+ T helper cells. $CD4^+$ T helper cells can be subclassified in Treg and effector T cells (Teffs). Teffs differentiate into various functionally distinct subtypes depending on the presented antigen, co-stimulatory signals, and the surrounding cytokine milieu [29]. The four best-studied subtypes are:

- Th1 cells are characterized by the expression of the transcription factor T-Bet and IFNγ production. Th1 cells physiologically combat intracellular pathogens like viruses and specialized bacteria.
- Th2 cells are marked by GATA-3 transcription factor expression and IL-4 production. They fight large extracellular pathogens like parasites.

- Th17 cells express the transcription factor RORγt and produce IL-17A+F. They defend against extracellular pathogens like most bacteria and fungi.
- TfH cells provide help to B cells in germinal centers during their activation, differentiation, and maturation [29].

Sometimes, T cells mistakenly target self-antigens, resulting in autoimmunity. A pathogenic role for autoreactive T helper effector cells in Lupus nephritis is well documented. In particular, crucial roles for pro-inflammatory Th1 and Th17, as well as TfH cells have been described. Autoreactive CD4 T cells were found to be expanding in active SLE patients, producing effector cytokines like IFNγ and IL-17 and infiltering in the kidney [30]. In Lupus nephritis, excessive production of inflammatory cytokines, such as IFNγ, and IL-17 is documented [31]. Furthermore, there's polarization of $CD4^+$ T cells towards pro-inflammatory Th1 and Th17 cells in SLE [32], [33]. This contributes to renal Fibrosis through the Th17/IL-17 axis [34], [35]. Functional evidence comes from mouse models. Mice lacking IL-17 production are protected from pristane-induced LN and develop fewer autoantibodies [36], [37]. Genetic ablation of CXCR3, a chemokine receptor that is mainly expressed on Th1 cells, resulted in decreased renal infiltration of these cells in Lupus-prone mice, resulting in amelioration of LN [38]. However, not only Th1 and Th17 cells show an important role in LN. Yamada et al. showed that $CCR4^+$ cells, also classified as Th2 cells are likely to migrate from the blood into the renal tissue of patients with LN [39]. This might be of functional importance since animals skewing toward a Th2 phenotype showed enhanced production of autoantibodies and deposition of IgG in the glomeruli [40].

Taken together, there is robust evidence, that Lupus nephritis is not solely driven by auto-antibodies produced by B cells. Rather, $CD4^+$ T effector cells also play a pivotal role in the disease pathogenesis via multiple mechanisms, including cytokine production and activation of macrophages, neutrophils, and B cells.

1.2.2. Tregs in LN

Tregs are crucial for maintaining self-tolerance [41]–[44]. The phenotypic hallmark of Tregs is the expression of the transcription factor forkhead box P3 (FoxP3) and the Interleukin 2 receptor alpha chain (CD25) [45]. Tregs execute their regulatory functions in various ways. Firstly, they can inhibit the function of other leucocytes

via soluble factors, for example, IL-10 [46], transforming growth factor beta (TGFβ) [47], and IL-35 [48]. Secondly, they utilize inhibitory receptors, which provide negative signals during T cell priming, including cytotoxic T lymphocyte antigen 4 (CTLA-4), and programmed cell death protein 1 (PD-1) [49]. Furthermore, they compete for growth factors like IL-2, which deprives Teff of this important proliferation and survival factor [49]–[51]. In addition, Tregs can secrete perforin and granzyme B, to directly induce cell death in activated Teff [52], [53]. Finally, Tregs bear ectonucleotidases on their surface, with which they can degrade danger signals like ATP in inflamed tissues [54].

In analogy to Teff, also numerous, functionally different Treg subtypes exist. In particular, the following subtypes are relevant in glomerulonephritis:

- Treg17 cells are programmed by STAT3 activation and are characterized by a $CCR6^+$ phenotype. Treg17 cells are specialized to suppress pathogenic Th17 responses, which has been shown to be of high relevance in acute and chronic glomerulonephritis in mice and humans.
- Treg1 cells are characterized by a $Tbet^+$, $CXCR3^+$ phenotype and are tailor-made to suppress pathogenic Th1 responses in autoimmune diseases like GN.
- $CCR7^+$ Treg: express CCR7 and lead to the immigration of Tregs into the renal draining lymph node. Here they suppress the activation of naïve $CCR7^+$ T helper effector cells.
- $ROR\gamma t^+$ Tregs: they are characterized by the expression of the hallmark transcription factor RORγt. They are the main subpopulation of Tregs infiltrating the kidney in the early stages of acute GN. They are metabolically highly active and display enhanced suppressive capacity [55].

A crucial role for Tregs in LN has been proven by multiple studies from the past. Depletion of $CD4^+CD25^+$ Tregs in a lupus-prone mouse model, as demonstrated by Hayashi et al. in 2005, resulted in increased immune complex deposition and aggravation of glomerulonephritis, underscoring the functional relevance of Tregs in the context of LN [56]. These findings are supported by Scalpino et al., revealing improved survival in the lupus-prone mouse model following the transfer of ex vivo expanded Tregs [57]. More recently, the specific roles of the different subsets of Tregs have become evident [55]. Our group emphasized the significance of Treg17 cells in protecting against LN in the pristane-induced model of SLE [58]. Not only

Treg17 cells showed importance during LN. Our group could also show, that RORγt$^+$ Tregs are essential for suppressing the type II response during LN [59]. Expanding beyond murine studies, investigations into human SLE patients revealed that mutations in the *FoxP3* locus, diminished Treg populations, and compromised functionality are all linked to SLE development [60]–[62]. Generally, Treg numbers were found to be reduced and less able to suppress in human patients with SLE, emphasizing their pathogenetic relevance [63]–[65]. In therapeutic interventions, low-dose IL2 therapy, which is crucial for Treg generation, survival, and function, led to Treg expansion and consequently reduced disease activity in SLE patients [66]. In conclusion, Tregs were shown to be crucial anti-inflammatory players in LN. Examining the precise functions and interactions of Tregs is therefore crucial for a better understanding of the disease and for developing new therapeutic approaches.

1.2.3. Monocyte/Macrophages

Monocytes/macrophages are important players of the innate immune system, that occur in nearly every tissue. Monocytes circulate in the blood and can extravasate and migrate into virtually any tissue of the body where they differentiate into tissue macrophages. Monocytes/macrophages fulfill diverse functions in the clearance of pathogens, as well as during sterile immune-mediated inflammation. One of their physiological roles is to phagocyte and kill pathogens, as well as infected cells. During sterile inflammation, they can be both, pro- as well as anti-inflammatory, depending on their status of differentiation [29].

The traditional differentiation of macrophage subclasses is classical macrophages, also called M1 macrophages, and alternatively activated macrophages (M2). M1 macrophages are induced by lipopolysaccharide (LPS) and IFNγ. They produce pro-inflammatory cytokines (IL-1β, tumor necrosis factor alpha (TNF-α)) and mediate tissue damage [29], [67]. M1 macrophages express the surface marker Ly6C (lymphocyte antigen 6 complex, locus 6) as well as the trafficking receptor CCR2 [29], [68], [69].

The anti-inflammatory M2 macrophages are induced by IL-4 and IL-13, they produce IL-10, and TGF-β and are therefore important in the wound healing process and the down-regulation of acute inflammation [70]. M2 macrophages downregulate CCR2 and Ly6C and can differentiate into tissue-resident macrophages with reparative and

anti-inflammatory properties [71]. M1 macrophages are postulated to be induced by Th1 cells, whereas the M2 macrophages seem to be activated by Th2 cells [67], [72]. Regarding renal inflammation, many studies from the past have documented important roles for both M1 and M2 macrophages in various experimental models of kidney diseases [73]–[75]. Concerning LN, the high prevalence of macrophages within renal tissues of nephritic mice as well as LN patients was documented in numerous studies [76]–[78]. Importantly, positive results of interventions interfering with monocyte and macrophage functions in mouse models of lupus nephritis have highlighted their significant role in LN progression [79]. Strategies targeting inflammatory macrophages [80]–[83], and efforts to induce an anti-inflammatory macrophage phenotype [84]–[86], have underscored the significant involvement of these cells in both acute and progressive forms of LN [79].

1.3. Renal fibrosis

If an inflammatory response persists for an extended duration and becomes chronically active, it triggers changes in the surrounding tissue. This leads to death and finally the replacement of the functional parenchyma by an extracellular matrix (ECM). This pathological change is called fibrosis and results in loss of organ function. Normally, when an acute injury occurs, a cascade of cellular and humoral mediators is activated to eliminate the infection or inflammatory stimulus to contribute to the wound healing of the injured tissue [29], [87].

Following tissue damage, injured epithelial and/or endothelial cells release inflammatory mediators and induce an antifibrinolytic coagulation cascade. Platelet degranulation leads to vasodilation and increased vascular permeability. Matrix metalloproteinases (MMPs) are produced by stimulated myofibroblasts, epithelial, and/or endothelial cells. These MMPs disrupt the basement membrane, facilitating the recruitment of inflammatory cells to the site of injury. Epithelial and endothelial cells secrete growth factors, cytokines, and chemokines that stimulate the proliferation and recruitment of leukocytes through the ECM. Neutrophils dominate the early inflammatory phase, followed by the recruitment of macrophages. They can clear the tissue from debris and dead cells, as well as eliminate invading organisms. Furthermore, macrophages and neutrophils produce cytokines and chemokines that enhance the wound-healing response. These factors also promote the migration and formation of new blood vessels by activated endothelial cells [88], [89]. Activated T

cells secrete profibrotic cytokines such as IL-13 and TGF-β, which further activates macrophages and fibroblasts. Fibroblasts transform into myofibroblasts, which contribute to wound contraction. Myofibroblasts can originate from local mesenchymal cells, and bone marrow (fibrocytes) or undergo epithelial-mesenchymal transition. In the final stages, epithelial and/or endothelial cells divide and migrate to regenerate damaged tissue, completing the normal healing process. However, in cases of repeated injury, chronic inflammation and repair lead to excessive accumulation of ECM components, as in lupus nephritis, resulting in the formation of a permanent fibrotic scar [87], [88], [90].

Fibrogenesis is facilitated by the continuous presence of a pro-inflammatory environment. The prolonged production of cytokines, angiogenetic factors, and growth factors results in a disparity between the myofibroblasts, responsible for producing ECM, and the MMPs responsible for its degradation [89], [91]. The accumulation of the ECM causes a replacement of the normal parenchyma with non-functional tissue, which therefore leads to irreversible damage of involved organs [90], [92].

A pivotal subset of immune cells of considerable relevance within the context of kidney fibrosis are macrophages. The normally anti-inflammatory M2 phenotype is driven towards a pro-fibrotic phenotype in chronic inflammation, in which recruitment and activation of myofibroblasts take place [93], [94]. These M2 macrophages persist in the kidneys and show a role in renal interstitial fibrosis, tubular injury, and collagen deposition [95]. Scaring of the glomeruli and tubular system leads to fewer working nephrons and decreased kidney function [96]. This causes renal dysfunction, and might finally result in ESKD [97]. The correlation between interstitial fibrosis and kidney function is undeniable [87], [96], [98]. The identification of factors involved in physiologic wound healing is therefore quite rewarding. Their stimulation or stabilization might represent novel therapeutic targets to prevent fibrosis and end-organ injury. One pivotal molecule in the balance between wound healing and pathogenic fibrosis is the multifunctional cytokine Amphiregulin (AREG), which binds to and signals via the epidermal growth factor receptor (EGFR).

1.4. The Amphiregulin/EGFR axis

The EGFR is involved in a variety of biological processes. There are seven known ligands of the EGFR: Transforming growth factor α (TGF-α), epidermal growth factor (EGF), heparin-binding EGF-like growth factor (HB-EGF), Epigen, Epiregulin, Betacellulin and Amphiregulin (AREG). Some of the ligands only have a low affinity to the EGFR (AREG; Epigen, Epiregulin), whereas the other ones have a high affinity to the receptor [99], [100]. Some of the ligands need to be activated from their membrane-bound form by a Metalloprotease called ADAM17 [101]. EGFR activation by its ligands plays a role in diverse biological processes, including cell proliferation, migration, differentiation, survival, and transformation [102]–[104]. It is known that activated EGFR plays a key role in many renal pathologies, including kidney regeneration after acute kidney injury [105], [106], as well as renal interstitial fibrosis and glomerular diseases [107]–[111]. The EGFR is upregulated in several renal cells, including podocytes, mesangial cells, and fibroblasts [112]. Besides the EGFR itself, also the ligands can be expressed in the kidney [113]. Studies in mice showed that the absence of HB-EGF as well as the EGFR itself on podocytes is protective against tissue damage in acute GN [112]. Patients suffering from LN showed increased HB-EGF expression, which might enhance kidney damage [114]. Besides HB-EGF, as described above, the EGFR has 6 other ligands and their role in LN needs to be unraveled.

One of these ligands, AREG, is known as a mediator of immunological processes, as well as of reparative effects within the tissue. Data suggest for example that AREG is a protecting factor against endothelial apoptosis and promotes endothelial cell proliferation and therefore enhances angiogenesis [115]. In particular, Minutti could show, that macrophage-derived AREG promotes the activation of TGF-β1 which leads to the differentiation of vascular pericytes into myofibroblasts and consequently to restitution of vascular integrity in wound healing [116]. Moreover, other studies showed the protective role of AREG secreted by macrophages in the context of experimental cardiac injury [117] and autoimmune uveitis [118].

In addition to macrophages, also Tregs were shown to secrete a high amount of AREG. Interestingly, Treg-derived AREG did not have effects on immunosuppression but rather enhanced repair of tissue damage of muscle cells after injury [119]. This observation led to the definition of so-called ´tissue repair´ Tregs.

Another cell type producing large amounts of AREG are innate lymphoid cell type 2 (ILC2). Evidence from two separate studies, one in a colitis model, and one in lung infection with influenza virus highlights the critical role of AREG production by ILC2s in mitigating tissue damage [120], [121]. Furthermore, Cao et al. emphasized the importance of ILC2s in protecting against kidney damage caused by ischemia. They found that silencing AREG in ILC2s worsened ischemia-induced fibrosis, highlighting AREG's protective role in mitigating renal tissue injury [122].

Another protective mechanism exerted by AREG was shown by Minutti in 2017. They unraveled AREG's pivotal role in defending against parasitic helminth infections. This mechanism involves sensitizing Th2 cells to IL-33 [123] and is of particular interest because Th2 immune responses can be protective in different forms of GN.

In addition to these tissue reparative functions, AREG has also been discovered to have strong immunosuppressive properties. Notably, it appears that AREG/EGFR interaction enhances the function of Tregs. In this context, AREG secretion by innate immune cells like macrophages, mast cells, and basophils stands out as a pivotal source of AREG, supporting the immunosuppressive capabilities of Tregs [118], [124], [125]. Our group recently showed that a complete knockout of AREG in the pristane-induced murine Lupus nephritis model leads to enhanced secretion of a broad spectrum of cytokines by $CD4^+$ T effector cells. As a consequence, AREG deficiency worsened the outcome of LN. Interestingly, EGFR signaling on Tregs was not involved in this AREG effect but rather a direct interaction of AREG with the EGFR on CD4+ effector T cells was required. Therefore, in addition to its non-immune mediated tissue reparative effects, AREG also plays a protective role by downregulating pro-inflammatory effector T-cell responses [126].

In contrast to the anti-inflammatory and tissue reparative functions of AREG, it can surprisingly also have a context-dependent pro-inflammatory and pro-fibrotic role. An increased AREG expression in keratinocytes leads to a psoriasis-like skin phenotype [127]. AREG also exerts pro-inflammatory functions in other autoimmune diseases such as rheumatoid arthritis, Sjögren syndrome, and allergic asthma. Several studies showed AREG as an initiator of the production of pro-inflammatory cytokines in the tissue which consequently leads to deterioration of the underlying disease [128]–[130]. In addition, our group recently showed that AREG potently induces pro-inflammatory macrophages (M1) and protects them from

apoptosis, which resulted in aggravation of renal injury in a model of acute glomerulonephritis [131]. In addition to these pro-inflammatory effects, AREG can also lead to increased fibrosis, which will be described in detail in the next chapter.

1.5. AREG in Fibrosis

Renal fibrosis, a key process in end-stage renal disease, involves the abnormal activation of renal fibroblasts and excessive extracellular matrix protein production. EGFR signaling has been shown to play a critical role in the development and progression of renal fibrosis. Lautrette et al. demonstrated that chronic Angiotensin II (Ang II) infusion caused renal interstitial fibrosis. Notably, these Ang II-induced effects were mitigated in mice overexpressing a dominant-negative EGFR construct [132]. Along the same line, in the context of unilateral ureteral obstruction (UUO)-induced renal fibrosis, researchers revealed that pharmacological EGFR inhibition or genetic reduction of EGFR activity substantially decreased the expression of α-smooth muscle actin and the deposition of fibronectin and collagen I in the kidney [107]. Furthermore, François et al. noted that using the EGFR inhibitor gefitinib efficiently stopped the progression of renal vascular and glomerular fibrosis [109].
Similar to the EGFR axis, its single ligands showed importance in renal fibrosis as well. Increased TGF-α, as well as its sheddase ADAM17, expression was observed in an Ang II-induced renal fibrosis model [132]. Furthermore, it was previously established that AREG plays a potent role in initiating liver fibrosis by modulating AREG-related mediators and growth factors [133]. Another study showed that AREG induces fibroblast proliferation and the expression of pro-fibrotic genes, which leads to lung fibrosis and an epithelial-mesenchymal transition in asthmatic mice [134]. AREG has also been shown to be highly expressed in the process of skin fibrosis, whereas AREG knockout mice showed less skin thickness and therefore are protected from bleomycin-induced skin fibrosis [135]. Furthermore, it was shown, that TGF-β leads to increased AREG expression, which as a result aggravated pulmonary fibrosis [136]. In alignment with this, AREG has been observed to be consistently secreted by renal tubule cells in various kidney diseases. Intriguingly, elevated AREG expression correlated well with the degree of fibrosis in cases of acute or chronic renal injury [101]. A subsequent study by different researchers further validated that AREG produced by proximal murine tubule cells (mPTC) indeed stands out as a primary initiator in the development of renal fibrosis.

Specifically, the targeted knockout of AREG in mPTCs proved protective against fibrosis in models involving UUO and ischemia-reperfusion, while also correlating with a reduction in infiltrating macrophages [137].

In summary, it is established that AREG plays a significant role in aggravating fibrosis within inflamed tissues, a process pivotal in the pathogenesis of end-stage renal diseases. According to the above-mentioned studies, it seems that AREG secreted by epithelial cell sources is responsible for the pro-fibrogenic effects. This contrasts with the anti-inflammatory and tissue reparative functions, which seem to be mediated by leukocyte-derived AREG.

Taken together AREG has multiple and partly opposing roles, which are strongly context-dependent and might differ according to the cellular source of AREG. This is summarized in Figure 2.

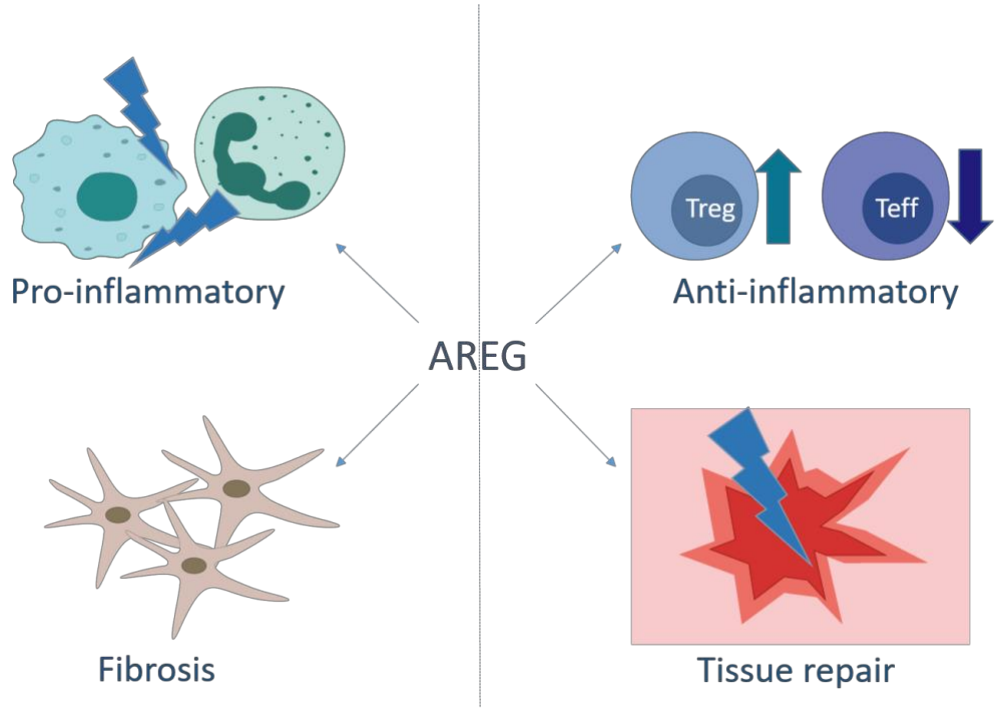

Figure 2: Overview of AREG-mediated effects

AREG is a multi-functional cytokine with pro-inflammatory properties via M1 macrophage activation, as well as fibrosis-promoting properties, leading to overactivation of fibroblasts. This contrasts with the anti-inflammatory functions, in which AREG enhances regulatory T cell (Treg) suppressive functions and can directly downregulate activated effector T cells (Teffs). Furthermore, AREG has enhancing effects on wound healing and tissue repair.

Based on the current data and as outlined in Figure 2, it is reasonable to speculate that the role of AREG may hinge on the specific cell type that releases it. In this context, it appears that AREG released from epithelial cells tends to have a pro-

inflammatory effect, whereas AREG originating from leukocytes exhibits a pro-regenerative and anti-inflammatory function. My thesis therefore aimed to investigate the cell-type-specific role of AREG derived from Tregs and macrophages in experimental lupus nephritis.

2. Material and Methods

2.1. Material

2.1.1. Equipment

Table 2-1: List of equipment

Equipment	Model	Manufacturer
Cellcounter	TC20	BioRad, Hercules, USA
Centrifuges	S424R	Eppendorf, Hamburg, Germany
	Multifuge X3R	Thermofischer Scientific, Waltham, USA
	Multifuge 1S-R	Eppendorf, Hamburg, Germany
Citadel	STP120	Thermofischer Scientific, Waltham, USA
ELISA Reader	MITRAS LB940	Berthold Technologies, Bad Wildbad, Germany
FACSymphony	A3	BD Biosciences, Heidelberg, Germany
gentleMACS Dissociator		Miltenyi Biotech B.V. & CO. KG, Bergisch Gladbach, Germany
Incubators	HeraCell	Heraeus Instruments, Hanau, Germany
Laminar flow benches	HERAsage	Heraeus Instruments, Hanau, Germany
Light microscopes	Axio Scope. A1	Carl Zeis AG, Oberkoch
Mikrotom	RM2255	Leica Mikrosysteme, Wetzlar, Germany
Nano Drop	DS-11 Sspectrophotometer	Denovix Inc., Delaware, USA

Pipettes	Pipetman P2, P10, P200, P1000	Gilson, Middleton, USA
Quant Studio	3 System	Thermofischer Scientific, Waltham, USA
Thermocycler	Biometra Trio	Analytik Jena, Jena, Germany
Vortex	Certomat MV	B.Braun Biotech, Melsungen, Germany
Water bath		GFL, Lauda-Königshofen, Germany

2.1.2. Consumables

Table 2-2: List of consumables

Material	Manufacturer
Counting Slides	BioRad, Hercules, USA
Disposable serological pipettes (5 mL, 10 mL, 25 mL, 50 mL)	Sarstedt, Nürnbrecht, Germany
FACS Tubes	Corning Incorporated, Corning, USA
FACS Tubes small	Corning Incorporated, Corning, USA
Filter normal 40 µm, 70 µm	Labsolute, Th. Geyer GmbH & Co. KG, Renningen, Deutschland;
Filter sort 40 µm, 70 µm	Corning Incorporated, Corning, USA
Gentle Macs C tubes	Miltenyi Biotech B.V. & CO. KG, Bergisch Gladbach, Germany
Histology tubes	Sarstedt, Nürnbrecht, Germany
Injekt-F 1 ml syringe	B. Braun SE, Germany
LS Columns	Miltenyi Biotech B.V. & CO. KG, Bergisch Gladbach, Germany
Pipette tips	Sarstedt, Nürnbrecht, Germany
Pipette tips, filtered	Sarstedt, Nürnbrecht, Germany
QPCR Plates	Sarstedt, Nürnbrecht, Germany
Reaction tubes	Sarstedt, Nürnbrecht, Germany

0.5 mL, 1.5 mL, 2.0 mL, 5.0 mL	
Reaction tubes **15 mL, 50 mL**	Sarstedt, Nürnbrecht, Germany
Slides	Invitro diagnostics, Sondheim, Germany
TC-Flask ventilated cap **T25, T75, T175**	Sarstedt, Nürnbrecht, Germany
Well plates **High-bind, conical, flat, round bottom**	Sarstedt, Nürnbrecht, Germany

2.1.3. Chemicals

If not otherwise clearly stated, all chemicals were bought from Carl Roth GmbH (Karlsruhe, Germany), Sigma-Aldrich Chemie GmbH (Steinheim, Germany), Merck KGaA (Darmstadt, Germany) or Roche Diagnostics GmbH (Penzberg, Germany).

Table 2-3: List of chemicals

Chemical	Manufacturer
Beta Mercaptoethanol	Gibco, LifeTechnologies, Billings, USA
Geltrex Membran	Gibco, LifeTechnologies, Billings, USA
Mouse serum	Biozol, Eching, Germany
NP-40	Abott Molecular Inc., Des Plaines, USA
Percoll	GE Healthcare Bio-Sciences, Uppsala, Sweden
vivid	Invitrogen by Life Technologies, Carlsbad, USA

2.1.4. Antibodies

Table 2-4: List of antibodies for flow cytometry

Antibody	Fluorochrome	Clone	Dilution	Manufacturer
AREG	Biotin	BAF989	1:200	R&D Systems, Minneapolis, USA

CD11b	PE-Cy7	M1/70	1:166	Biolegend, San Diego, USA
CD11c	APC	N418	1:125	Biolegend, San Diego, USA
CD19	BV450	6D5	1:111	Biolegend, San Diego, USA
CD3	AF700 BV785	17A2	1:111 1:200	Biolegend, San Diego, USA
CD4	APC-Cy7	RM4-5	1:111	BD Biosciences by Benson & Dickinson, Franklin Lakes, USA
CD44	BV785	IM7	1:333	Biolegend, San Diego, USA
CD45	PerCP	30-F11	1:111	Biolegend, San Diego, USA
CD62L	BV605	MEL14	1:125	Biolegend, San Diego, USA
CD69	PE-Cy7	H1.2F3	1:125	BD Biosciences by Benson & Dickinson, Franklin Lakes, USA
CD8	BV650	56-6.7	1:333	Biolegend, San Diego, USA
FoxP3	FITC APC	FJK-16s	1:125	Invitrogen by Life Technologies, Carlsbad, USA
γδTCR	BV510	eBio GL3	1:125	Biolegend, San Diego, USA
IFNγ	APC	XMG1.2	1:166	eBioscience, San Diego, USA
IL-10	PE	JES5-16E3	1:125	Biolegend, San Diego, USA
IL-13	BV450	eBio13a	1:100	Invitrogen by Life Technologies, Carlsbad, USA

IL-17A	BV605	TC11-18H10	1:166	Biolegend, San Diego, USA
Ki67	BV450	B56	1:100	BD Biosciences by Benson & Dickinson, Franklin Lakes, USA
Ly6C	FITC	AL-21	1:285	BD Biosciences by Benson & Dickinson, Franklin Lakes, USA
Ly6G	APC-Cy7	1A8	1:200	Biolegend, San Diego, USA
MHCII	BV510	N5/114.15.2	1:666	Biolegend, San Diego, USA
Rorγt	PE	Q31-378	1:666	BD Biosciences by Benson & Dickinson, Franklin Lakes, USA
Streptavidin	BV785		1:200	BD Biosciences by Benson & Dickinson, Franklin Lakes, USA
TNFα	PE-Cy7	MP6-XT22	1:125	Biolegend, San Diego, USA

Table 2-5: List of antibodies for histology

Antibody	**Clone**	**Manufacturer**
C3	A0062	Dako, Hamburg, Germany
Caspase 3 (Asp175)	5A1E	Cell Signaling Technologies, Danves, USA
mIgG	polyclonal	Dianova, Hamburg, Germany
Polymer-based secondary antibody alkaline phosphatase kit		POLAP; Zytomed, Berlin, Germany

2.1.5. Kits

Table 2-6: List of kits

Kits	Manufacturer
Annexin V	Biolegend, San Diego, USA
AREG ELISA	R&D Systems, Minneapolis, USA
CD4 Microbeads Kit	Miltenyi Biotech B.V. & CO. KG, Bergisch Gladbach, Germany
IFNγ ELISA	Biolegend, San Diego, USA

2.1.6. Cell lines

Table 2-7: List of cell lines

Cell line	Description	
hGEnC	Human glomerular Endothelial cells	Simon C Satchell, Bristol Medical School, Bristol, United Kingdom.
mMC	Murine Mesangial cells	AG Panzer, UKE, III. Nephrology
mTC	Murine Tubular cells	AG Panzer, UKE, III. Nephrology

2.1.7. Media and recombinant proteins

Table 2-8: List of media and recombinant protein for cell culture

Media and recombinant Proteins	Manufacturer
Digest-Medium	RPMI, 5% FCS, 1% P/S, 1%HEPES
DMEM	Gibco, LifeTechnologies, Billings, USA
EGM™-2 Endothelial Cell Growth Medium-2 BulletKit™	Lonza AG, Basel, Switzerlang
Recombinant human AREG	R&D Systems, Minneapolis, USA
Recombinant murine AREG	R&D Systems, Minneapolis, USA

X-VIVO™ Medium	Biozym Scientific; Hessisch Oldendorf, Germany

2.1.8. Buffer and solutions

Table 2-9: List of buffer and solutions

Buffer/Solution	Manufacturer
Digest Media	
Erylysis Stock 1	Tris(hydroxymethyl)aminomethane at pH 7.6 in H2O
Erylysis Stock 2	144mM ammonium chloride in H2O
FCS	Gibco, LifeTechnologies, Billings, USA
HBSS	Gibco, LifeTechnologies, Billings, USA
HEPES	Gibco, LifeTechnologies, Billings, USA
Lysis Buffer	20 mL 0,5 M Tris pH 8,5 20 mL 1 M NaCl 1 mL 0.5 M EDTA 2 mL 10 % SDS Add 100 mL dest H_2O
MACS Buffer	Miltenyi Biotec; Bergisch Gladbach, Germany
PBS	Gibco, LifeTechnologies, Billings, USA
Penicilin/Streptavidin	Calbiochem®, Sigma-Aldrich; St. Louis, MO, USA
RPMI	Gibco, LifeTechnologies, Billings, USA
Sodium Pyruvat	Gibco, LifeTechnologies, Billings, USA
Trypsin	Gibco, LifeTechnologies, Billings, USA

2.1.9. Mice

Table 2-10: List of used mice

Mice	
FoxP3^{cre} x AREG$^{fl/fl}$	B6.129$^{(Cg)-Foxp3tm4(YFP/icre)Ayr/J - Aregtm2a(EUCOMM)Hmgu}$
LysM^{cre} x AREG$^{fl/fl}$	B6.129P2$^{Lyz2tm1(cre)Ifo/J -Aregtm2a(EUCOMM)Hmgu}$

2.1.10. Software and databases

Table 2-11: List of software and databases

Software/databases	**Application**	**Manufacturer/Source**
Adobe Illustrator	Design of the graphics	Adobe
Angiogenesis Analyzer PlugIn for FIJI	Analysis for angiogenesis in hGEnC	Gilles Carpentier
FIJI	Image processing program	ImageJ
FlowJo	Single-cell flow cytometry analysis	BD Biosciences
GraphPad Prism	Data presentation and statistical analysis	GraphPad Software, Inc.
QuantStudio Design & Analysis Software	Analysis of QPCR Data	Applied Biosystems
Wound Healing PlugIn for FIJI	Analysis of the scratch assay	Alejandra Suarez-Arnedo

2.2. Methods

2.2.1. Human glomerular endothelial cells

An immortalized human glomerular endothelial cell line (hGenC) was kindly provided by Professor Simon C Satchell, Bristol Medical School, Bristol, United Kingdom. Primary hGEnC were immortalized by transfection with the SV-40 virus [138]. hGEnC were cultured in EGM™-2 Endothelial Cell Growth Medium-2 at 5 % CO_2 and 33 °C. To perform cell culture experiments, cells were trypsinized, counted, and seeded in a 6-well plate at a density of 3.0×10^5 cells/well.

2.2.2. Murine proximal tubules and mesangium cells

Mouse kidney proximal tubule cells (mTC) are derived from a cell line obtained by microdissection from the mouse proximal tubule which was immortalized by transformation with the SV-40 virus [139]. Mouse mesangium cells (mMC) were initially obtained from mouse kidneys by differential sieving and digestion techniques and also immortalized by transformation with the SV virus [140]. Cells were cultured in DMEM medium containing 10 % FCS, 100 U/mL penicillin, 100 mg/mL streptomycin at 37 °C, and 5 % CO_2. Confluent mTC and mMC were solubilized for cell culture experiments using trypsin and seeded in a 6-well plate at a dilution of 1:10 for mMC and 1:15 for mTC. cells were incubated in serum-free DMEM for 24 hours before stimulation.

2.2.3. Scratch-assay

For the scratch assay, cells were seeded in 6 well plates as described above and cultured at 5% CO_2 and 37 °C for an additional 1-2 days until they grew confluent. Then, the respective wells were scratched longitudinally with a 100 µL pipette tip. The medium was removed, and fresh medium was used with or without the addition of 50 ng/mL recombinant human or murine AREG. For evaluating scratch closure, images were taken using an inverted microscope at time 0h. Cells were then further cultured at 5 % CO_2 and 37 °C for an additional 6h in the case of hGEnC and 48 h in the case of mMC and mTC, after which images were again taken using an inverted microscope. Wound healing was then determined using a wound healing analysis plug-in for ImageJ.

2.2.4. Endothelial-tube-formation-assay

The endothelial tube formation assay quantifies the capacity of endothelial cells to generate capillary-like structures (tubes). Therefore, the cells are seeded subconfluently and supported by an extracellular matrix. A 24-well plate was coated with GeltrexTM matrix and allowed to cure at 37 °C for 30 min. 7.5×10^4 hGEnC were mixed with medium, with or without 50 ng/mL recombinant human AREG, 300 µL of this mixture was added to each well and cultured at 5 % CO_2 37 °C for 30 h. Images were then acquired using an inverted microscope and quantified for tube formation using an Angionese Analyzer PlugIn in ImageJ.

2.2.5. Animal experiments

For the lupus nephritis model, 8–12-week-old female mice of the indicated genotypes were injected intraperitoneally once with 500 µL of pristane oil (2,6,10,14-tetramethylpentadecane). For analysis of pristane-induced peritonitis, mice were killed after 7-14 days, whereas chronic lupus nephritis occurs after approximately 12 months; therefore, animals were killed 12-15 months after pristane injection.
Animal experiments were performed according to national and institutional animal welfare and ethics guidelines and approved by local committees (N081/2020, N21/005).

2.2.6. Leucocyte isolation from tissue

The spleens were collected and pushed through a 70 µm nylon sieve containing Hanks' Balanced Salt Solution (HBSS). Erythrocytes were lysed using ammonium chloride. The cells were subsequently washed and passed through a 40 µm nylon sieve. Cell numbers were counted using an automated cell counter. For isolation of leukocytes from kidneys, these were minced and placed in a digestion medium at 37 °C for 45 min and then dissociated using a gentleMACS^{TM} dissociator. A 37 % Percoll gradient was run for further purification.

2.2.7. Flow cytometry

The cell suspension of the organs from individual animals was centrifuged for 5 min at 350 g at 4 °C. To block unspecific binding, the cells were incubated for 20 min with 10 % mouse serum and then centrifuged at 360 g for 2 min. After blocking, the cells were treated for 20 min at 4 °C with fluorochrome-labeled antibodies against

CD45, CD3, γδTCR, CD4, and CD8 to analyze T cells. To check the monocytes and macrophages, the cells needed to be surface stained with CD45, CD3, CD19, CD11b, CD11c, Ly6C, and Ly6G. The gating strategy is shown in Figures 3 and 4. Any in-depth information on the used antibodies and dilutions can be found in Table 2-4. After the surface staining, the cells were washed with PBS and stained with vivid, live-dead dye. For intracellular staining, cells were fixed in 3.65 % paraformaldehyde (PFA) for 20 min at room temperature (RT) and then permeabilized with 0.1 % Nonidet P-40 for 4 min at RT. Fluorochrome-labeled antibodies against IL-10, IL-17, IFNγ, TNFα, IL-13, Ki-67, and FoxP3 were used for intracellular/intranuclear staining. For intracellular AREG staining, we used a biotinylated anti-AREG antibody followed by fluorochrome-labeled streptavidin. For ex vivo cytokine stimulation, cells were activated with phorbol-12-myristate-13-acetate (PMA) (50 ng/mL), ionomycin (1 µg/mL), and brefeldin A (10 µg/mL) for 2.5 h at 37 °C. Experiments were performed using a BD FACSymphony A3.

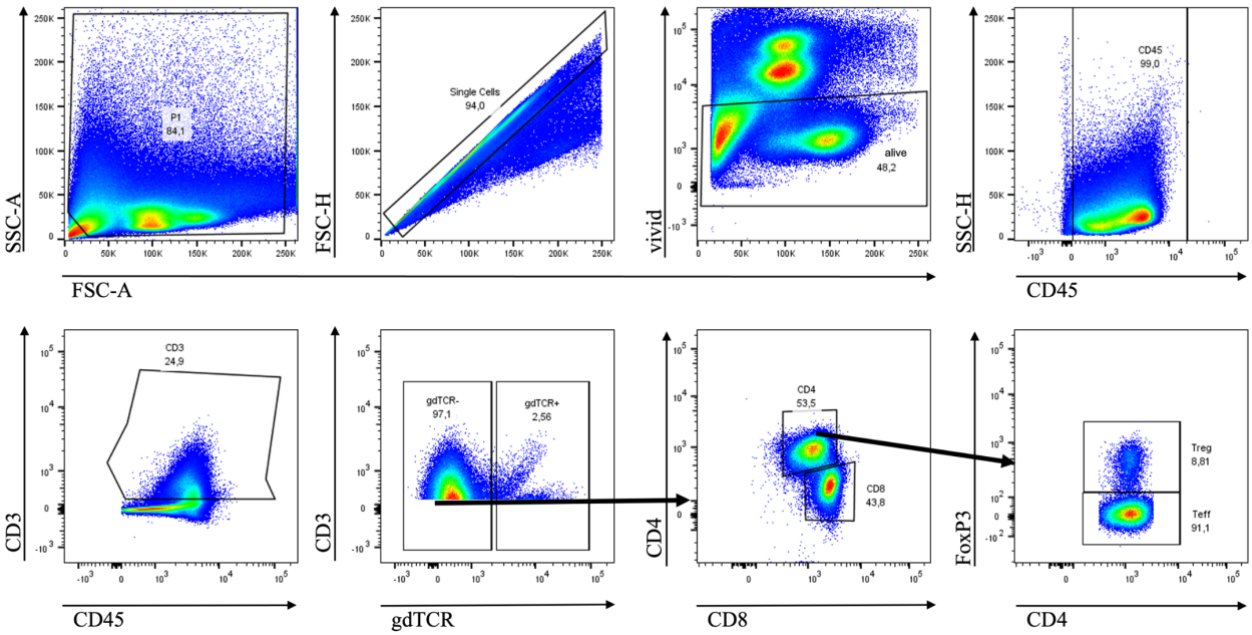

Figure 3: Gating strategy for CD4$^+$ Teffs and Tregs

Spleen cells from WT mice at 12 months after pristane-induced LN are shown as an example. First, the debris was gated out using FSC-A and SSC-A. Afterward, the single cells were gated using FSC-H and FSC-A. Dead cells were excluded using a live-dead dye (vivid). Lymphocytes were then gated with the surface marker CD45 and afterward, the CD3$^+$ stained T cells were identified. To exclude γδT cells the surface marker γδ TCR was stained, and negative cells were gated and further checked for CD4 and CD8. The CD4$^+$ T-cells were then checked for FoxP3 expression for identification of regulatory T cell (Tregs), whereas FoxP3^{neg} T-cells were labeled as effector T cells (Teffs).

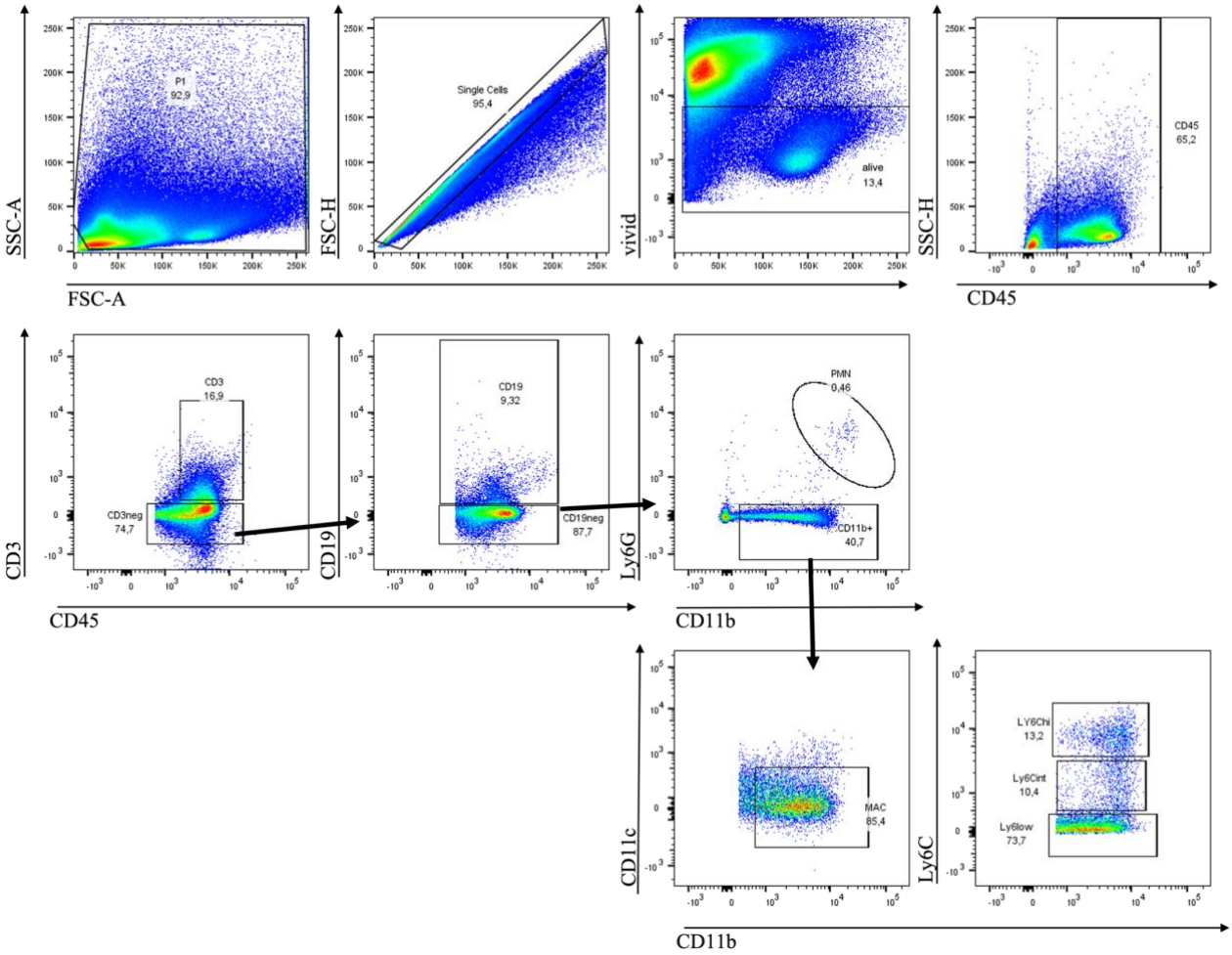

Fig.4: Gating strategy for PMN, M1 and M2 macrophages

Kidney cells from WT mice at 12 months after pristane-induced LN are shown as an example. First, the debris was gated out using FSC and SSC. Afterward, the single cells were gated using FSC-H and FSC-A. Dead cells were excluded using a live-dead dye (vivid). Lymphocytes were then gated with the surface marker CD45 and afterward, T cells and B cells were excluded via CD3 and CD19 staining. After excluding the lymphocytes, the cells were tested for the surface markers Ly6G and CD11b. $Ly6G^{+}$ and $CD11b^{+}$ cells were labeled as polymorphonuclear neutrophils (PMN). $CD11b^{+}$ $Ly6G^{neg}$ cells were tested for CD11c. The CD11c negative population was labeled as macrophages. For testing the polarization of the macrophages, the cells were stained for Ly6C. $Ly6C^{high}$ macrophages were labeled as M1, whereas $Ly6C^{low}$ Macrophages were labeled as M2.

2.2.8. Annexin V-staining

To detect apoptotic cells, staining with Annexin V was performed. Cells were stained as described above in the chapter 'flow cytometry'. After live-dead staining, cells were resuspended in BioLegend Annexin V buffer containing a 1:50 dilution of Annexin V antibody, washed in BioLegend Annexin V Buffer, and immediately analyzed by flow cytometry.

2.2.9. Sorting

For experiments using primary mouse T cells, cells were isolated using a FACS-Sorter. Single-cell suspensions were prepared from spleens as described above and stained with antibodies against B cells (CD19) and T cells (CD3 and CD4) to isolate specific leukocyte populations. Fluorescence emitted from the FoxP3$^{cre/yfp}$ construct was used to identify and sort Tregs.

2.2.10. Genomic DNA experiments

Sorted cells were suspended in 200µL lysis buffer (Table 2-9) containing 1:100 Proteinase K. The suspension was put in a 55 °C warm thermoblock for 1 h and afterward centrifuged for 10 min at 12000 rpm at RT. The supernatant was collected and transferred into a tube containing 200 µL isopropanol. The tube was inverted until the DNA was precipitated and centrifuged for 10 s at 4000 rpm at RT. Then, the DNA was washed 2 times with 500 µL 70% EtOH, and after each washing step centrifuged for 10 s at 4000 rpm RT. In the last step, the DNA was centrifuged for 10 min at 4000 rpm RT. The supernatant was discarded, and the DNA was dried at RT for about 15 min. The dried DNA was resuspended in 50 µL H_2O and heated in a 55 °C thermoblock for 1 h. For the PCR analysis, the DNA concertation was measured using a nanodrop, and equal amounts were used. The protocol for the PCR is shown in Table 2-12 and the temperature profile is shown in Table 2-12. The PCR products were analyzed on a 2 % TBE-agarose-ethidium-bromide-gel under UV Light.

Table 2-12: Protocol for AREG PCR

	amount per attempt
Areg flox incl. Intron 4 for	1 µL
Areg flox incl. Intron 4 rev	1 µL
dNTPs(10mM each)	0.4 µL
10 x DreamTaq-Puffer	2 µL
H2O	14.5 µL
Dream-Taq	0.1 µL

Table 2-13: Temperature profile

Temperatur	**Time**		**Cycles**
95 °C	3 min		
95 °C	30 s		
60 °C	30 s		
72 °C	1 min	Go to step 2	30
72 °C	5 min		
4 °C	hold		

Table 2-14: Primer

Primer	**Sequence**
Areg flox incl. Intron 4 for	CCA AAC CCT CTC AAC GCA CT
Areg flox incl. Intron 4 rev	GCG AGG ATG ATG GCA GAG AC

2.2.11. Murine ELISA analysis

Retrobulbar blood was collected in ethylenediaminetetraacetic acid (EDTA) coated tubes, and centrifuged at 3500 rpm, 4 °C for 15 min. The cells were discarded, and the plasma was used for further analysis. ELISA was performed at the indicated dilutions after coating the microtiter plates with poly-L-lysine and calf thymus DNA to analyze circulating anti-ds DNA antibodies from the plasma. For analysis of total

non-antigen-specific immunoglobulins, ELISA plates were pre-coated with anti-mouse IgG antibodies. Anti-total IgG was used as a secondary antibody. ELISA for anti-U1-snRNP in the plasma was performed at the indicated dilutions after coating the microtiter plates with snRNP.

2.2.12. Histological staining

The formaldehyde-fixed kidney tissue was washed with PBS and then dehydrated using ethanol, xylol, and paraffin for histological analysis. The tissue was poured into paraffin blocks and after drying cut into 1-3 µm thin slices and pulled onto uncoated slides. The slides were baked at 40 °C for better adhesion. Histological staining was performed in aqueous solutions; therefore, the sections needed to be deparaffinized by a descending alcohol series starting with xylol.

2.2.13. Periodic acid Schiff staining (PAS)

After deparaffinization 2 µm thin sections were immersed in a 1 % periodic acid solution, followed by staining for 40-60 min in Schiff's reagent, which mainly stains glycoproteins, mucins, and glycogen. This was followed by nuclear staining with hemalaun according to Böhmer. After ascending alcohol series, the sections were cover-slipped with Eukit. The nuclei are stained blue, PAS-positive structures are bright red, and the remaining tissue is pale pink.

2.2.14. Assessment of renal histological changes

The semiquantitative evaluation of renal histological damage was performed for the most part by the medical laboratory attendant. The PAS-stained sections were scanned for glomerular damage and tubulointerstitial injury. The tubulointerstitial injury was characterized by features such as tubular dilation, atrophy, sloughing of tubular epithelial cells, tubular basement membrane thickening, and interstitial inflammation. Following the grading system introduced by Phoon et al. in 2008 [141], the injury level was categorized on a scale from 0 to 4: grade 0 indicating no tubulointerstitial injury and no interstitial inflammation, and subsequent grades reflecting increasing severity with percentages of tubulointerstitial injury and inflammation [141]. Semiquantitative scoring of the tubulointerstitial damage was performed using 20 randomly selected cortical areas (×200). The mean glomerular area was measured by assessing a minimum of 50 randomly selected glomeruli from

high-power images (magnification x400) using AxioVision Rel. 4.8 LE [142]. Glomerular abnormalities were evaluated in a minimum of 50 glomeruli per mouse in 1.5 µm thick PAS-stained sections as published elsewhere [143]. These assessments encompassed various features such as glomerular hypercellularity, crescent formation, fibrinoid necrosis, hyalinosis, capillary wall thickening, and segmental proliferation.

2.2.15. Fibrosis staining

For staining fibrotic tissue, 3 µm thin kidney sections embedded in paraffin were stained with Sirius Red for 1 h. After washing, the sections were stained with Fast Green for 1 h. After an ascending alcohol series, the sections were cover-slipped with Eukit. Images of the slides were taken randomly. Images were analyzed for red staining using ImageJ.

2.2.16. Immunohistology staining

For analysis of renal immune complex depositions, paraffin-embedded sections were stained with antibodies directed against complement component 3 (C3), cleaved caspase-3, or mouse immunoglobulin G (mIgG) and developed with a polymer-based secondary antibody alkaline phosphatase kit. Positive cells in 50 glomerular cross-sections and 20 tubulointerstitial high-power fields (magnification ×400) per kidney section were counted in a blinded manner.

2.2.17. Immunohistology staining of human renal biopsies

The immunostaining was performed by our collaboration partners from the INSERM in Paris, France. The detailed methods are described in our publication [126].

3. Results

3.1. AREG expression is increased in human lupus nephritis

In a recent publication by our group, we could show that AREG exerts a protective effect against LN via broadly downregulating pathogenic $CD4^+$ Teff response. In this publication, we, and our collaboration partners from the INSERM in Paris, France reported, that AREG exhibits only minimal expression in kidneys from healthy controls, whereas significant upregulation of AREG expression was observed in biopsies of LN patients with class III/IV. Figure 5 illustrates the multiplexed immunofluorescence analysis of these patients' samples. Using different markers, we could identify the leucocyte sources of the AREG expression. Quantification of the staining showed significant AREG expression by $FoxP3^+$ $CD4^+$ cells, as well as $CD68^+$ cells (Fig. 5b), indicating Tregs, as well as monocytes/macrophages as the primary producers of AREG [126].

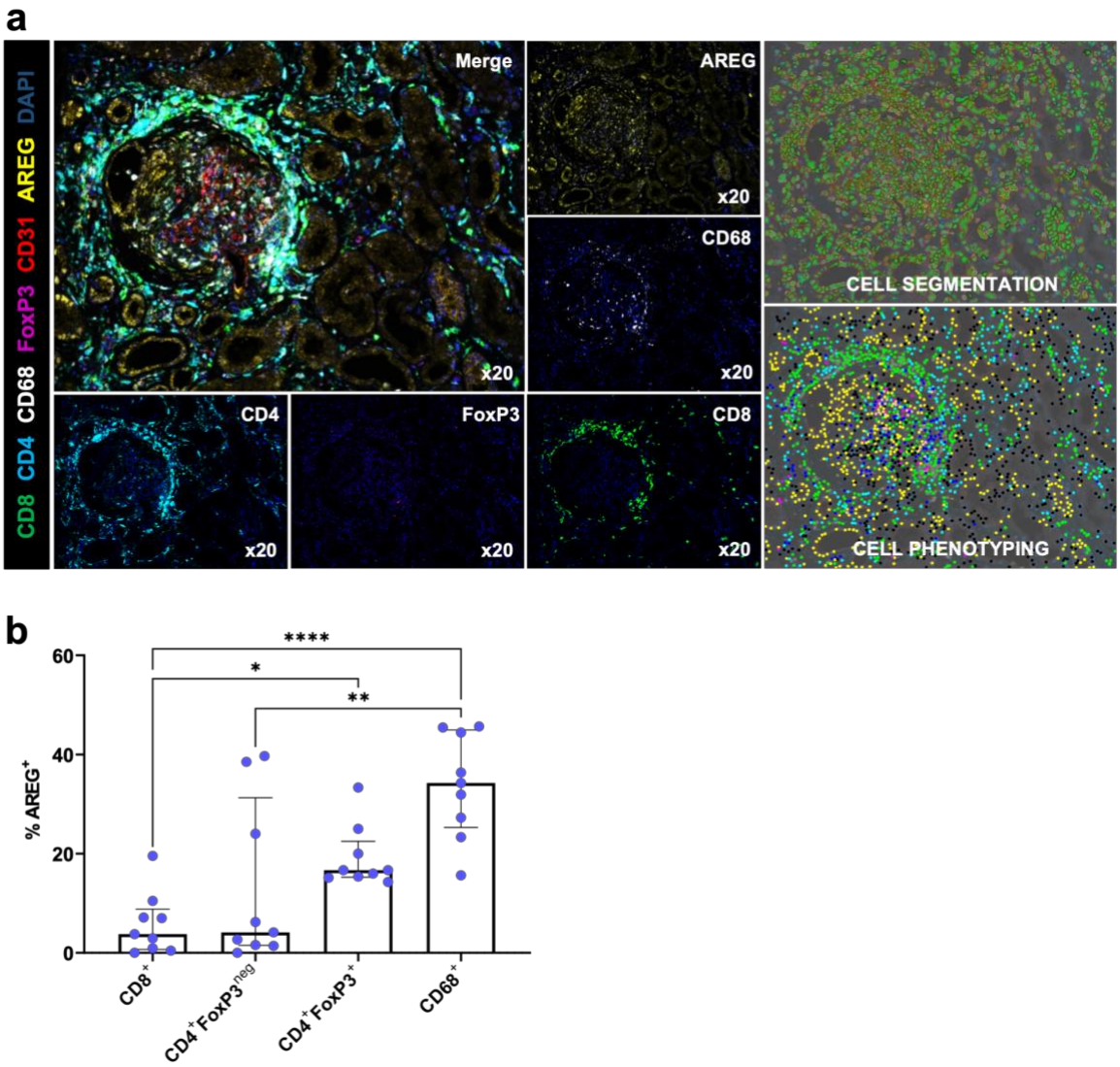

Figure 5. AREG expression is increased in renal infiltrating leukocytes of patients with LN

(a) Multiparametric immunofluorescence staining of AREG expression in renal infiltrating macrophages ($CD68^+$), regulatory T cells ($CD4^+FoxP3^+$), as well as $CD4^+$ and $CD8^+$ effector T cells ($CD4^+FoxP3^{neg}$ and $CD8^+$ resp.) (x20 magnification). Representative examples of automated cell segmentation and phenotyping according to marker expression are shown. (b) Quantification of the percentage of AREG-expressing cells within the indicated leukocyte cell types. Symbols represent individual patients, bars represent median values and interquartile range. *p<0.05, **p<0.01, ****p<0.0001. The figure is a modified version of the publication by Melderis et al. [126].

Building on these findings, we aimed to initiate a more in-depth investigation into the cell type-specific role of AREG expressed by Tregs and macrophages.

3.2. Generation of mice with Treg-restricted deficiency of AREG

As explained above, our recent investigations have revealed that a pan knockout of AREG results in aggravation of nephritis in the pristane-induced LN mouse model. As a mechanism, we could identify that AREG directly downregulates pathogenic Teff activation and their cytokine production. Detailed analyses have revealed that AREG can be produced in this experimental model, as well as in human LN, by different cellular sources. Since many studies from the past have shown differential and often opposing roles of AREG depending on the cellular origin, my thesis set off to examine the cell type-specific role of AREG in LN.

Since our results had shown, that one of the major renal leukocyte sources of AREG in the pristane model of LN as well as in humans are Tregs, we intercrossed mice expressing cre recombinase under the control of the FoxP3 promotor with mice bearing a loxP flanked AREG gene. This resulted in mice with Treg-restricted AREG deficiency, which will be referred to as $FoxP3^{cre}$ x $AREG^{fl/fl}$ mice. To confirm the successful excision of AREG in Tregs, I sorted B cells, Teffs, and Tregs from $FoxP3^{cre}$ x $AREG^{fl/fl}$ mice and isolated genomic DNA for PCR analysis, using primers designed to bind upstream of exon 4. In Figure 6a the allele structure of the $AREG^{fl/fl}$ mice ($Areg^{tm2a(EUCOMM)Hmgu}$) is shown. The critical exons for the expression of AREG are exons 3 and 4. When the cre recombinase under the control of the FoxP3 promotor is activated, the loxP flanked exons 3 and 4 are excised and a DNA strand without exons 3 and 4 is created (Fig. 6b). Tregs, that express FoxP3, are therefore not able to produce AREG anymore. To investigate if the cre-flox system is working properly, I designed primers (Table 2-14) binding in the intron before exon 4 and directly in the exon 4, as shown in red arrows (Fig. 6a). Therefore, if the cre-flox-system is working properly, the resulting PCR product with a size of 455bp (Fig. 6b) is missing only in Tregs.

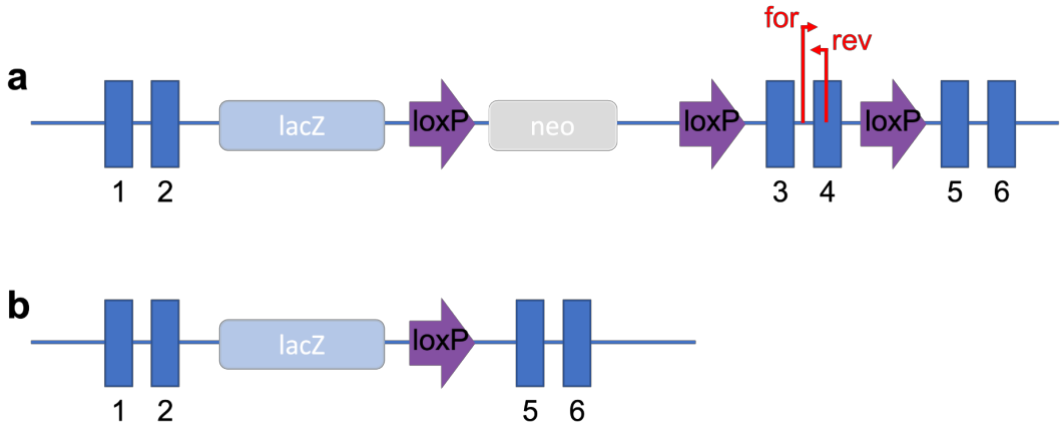

Figure 6: Genetic modification of AREG$^{fl/fl}$ mice
(a) The genomic structure of the Areg$^{tm2a(EUCOMM)Hmgu}$ mouse with a floxed AREG gene Adapted from the IMPC website (www.mousephenotype.org), this figure was crafted based on the information available on the site. Exons are numbered 1-6 and indicated by blue bars. LacZ (lacZ) and neomycin genes (neo) are shown as light blue and grey rectangles respectively. The three floxed (loxP) sites are shown by dark purple arrows. The position of the primers used in our analyses is marked by red arrows with the forward (for) primer binding within the intron between exons 3 and 4 and the reverse (rev) primer binding within exon 4. (b) The expected genomic structure after cre-mediated recombination with excision of the critical exons 3 and 4.

As illustrated in Fig. 7a I observed a significantly reduced PCR band intensity specifically in genomic DNA from the sorted Treg population in comparison to genomic DNA from Teffs and B cells. Notably, relevant AREG excision did also not occur in non-lymphoid tissues as evidenced by identical bands using genomic DNA from tail tips of wildtype and FoxP3^{cre} x AREG$^{fl/fl}$ mice. To validate this finding on the protein expression level, I performed ex vivo spleen and kidney cell stimulation from FoxP3^{cre} x AREG$^{fl/fl}$ and control mice at 15 months of pristane-induced LN, followed by staining for AREG. In both the spleen and the kidney, AREG expression in Tregs was almost absent in FoxP3^{cre} x AREG$^{fl/fl}$ mice. Figure 7b shows a representative FACS-Plot, Figure 7c the quantification of AREG^{+} Tregs in the kidney, and Figure 7d in the spleen. Another cell type known to produce AREG are γδT cells, so these were used as controls. In contrast to Tregs, AREG expression by γδT cells remained unchanged in FoxP3^{cre} x AREG$^{fl/fl}$ mice (Fig. 7e-g). In summary, my data show, that the deficiency of AREG in our newly generated mice is indeed limited to Tregs.

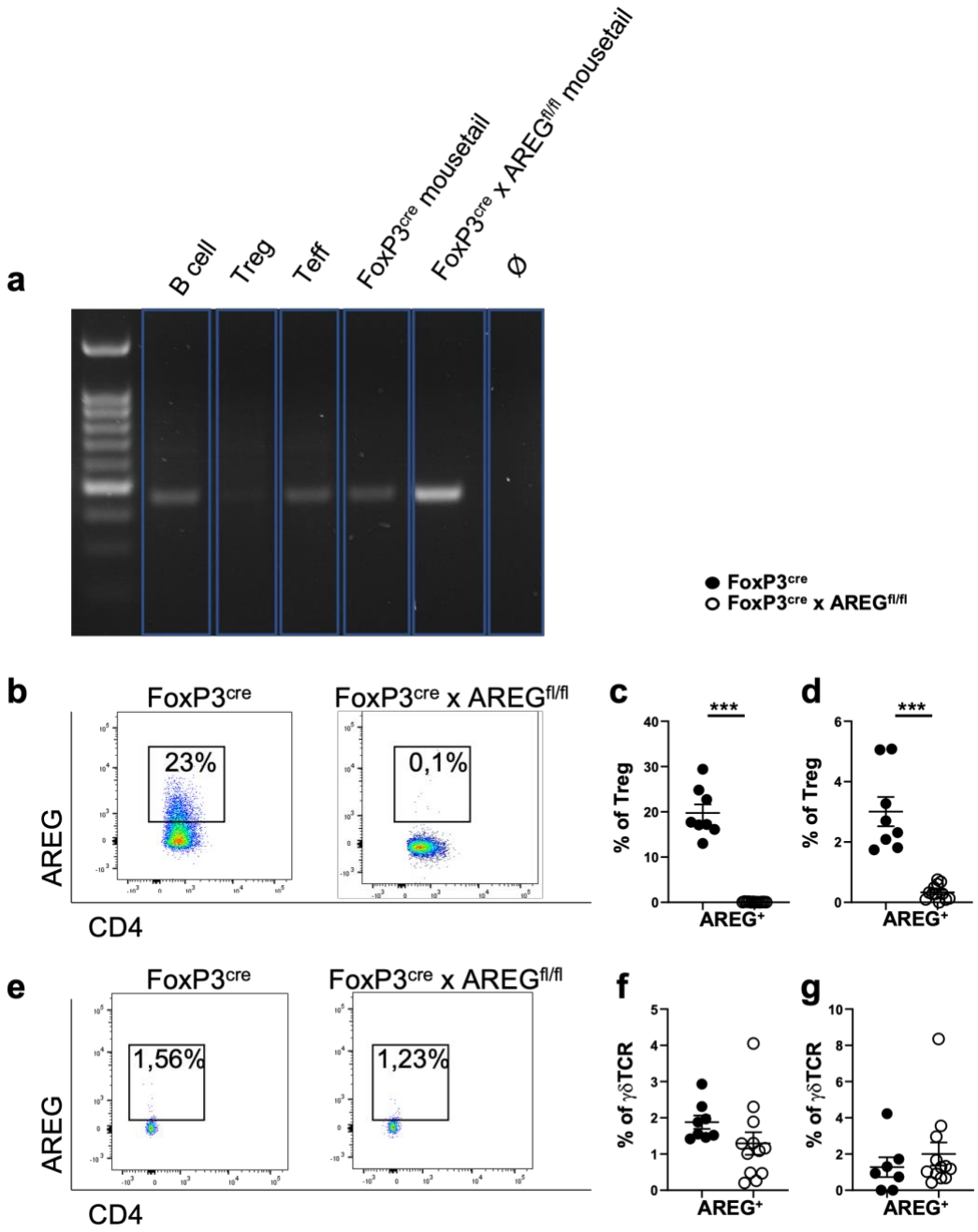

Figure 7: Lack of AREG in FoxP3^{cre} x AREG$^{fl/fl}$ mice is limited to Tregs

(a) PCR analysis of the AREG gene from genomic DNA from highly purified splenic B cells, regulatory T cells (Tregs), and effector T cells (Teffs) of FoxP3^{cre} x AREG$^{fl/fl}$ mice, and of tail tissue from wildtype mice and FoxP3^{cre} x AREG$^{fl/fl}$ mice. (b) Representative FACS plot of AREG^{+} Tregs in the spleen of mice at 15 months of pristane-induced lupus nephritis (LN). (c-d) Quantification of AREG^{+} Tregs in (c) the spleen and (d) the kidney of mice with the indicated genotype treated with pristane for 15 months. (e) Representative FACS plot of AREG expression by γδTCR^{+} T cells in the spleen of control mice. (f-g) AREG^{+} γδT cells in (f) spleen and (g) kidney of mice with the indicated genotype at 15 months of pristane-induced LN. Symbols show individual animals, horizontal lines show mean values. Error bars show the standard error of the mean. ***$p<0.001$

3.3. Deficiency of AREG in Tregs leads to a worsened renal outcome of pristane-induced LN after 12 months

After demonstrating selective AREG deficiency in our newly generated FoxP3^{cre} x AREG$^{fl/fl}$ mice, we aimed to investigate the role of Treg-derived AREG in LN. Therefore, LN was induced by intraperitoneal pristane injection into female mice aged 10-12 weeks. After 12 months, we examined kidney histology, which showed aggravation of LN in FoxP3^{cre} x AREG$^{fl/fl}$ mice as compared to FoxP3^{cre} controls. This was evidenced by a significant increase in histologically abnormal glomeruli (Fig. 8a, b) and increased glomerular area in mice lacking AREG in Tregs (Fig. 8c). Notably, the damage was largely limited to the glomeruli, with only a trend towards more damage in the renal interstitium of FoxP3^{cre} x AREG$^{fl/fl}$ mice (Fig. 8d).

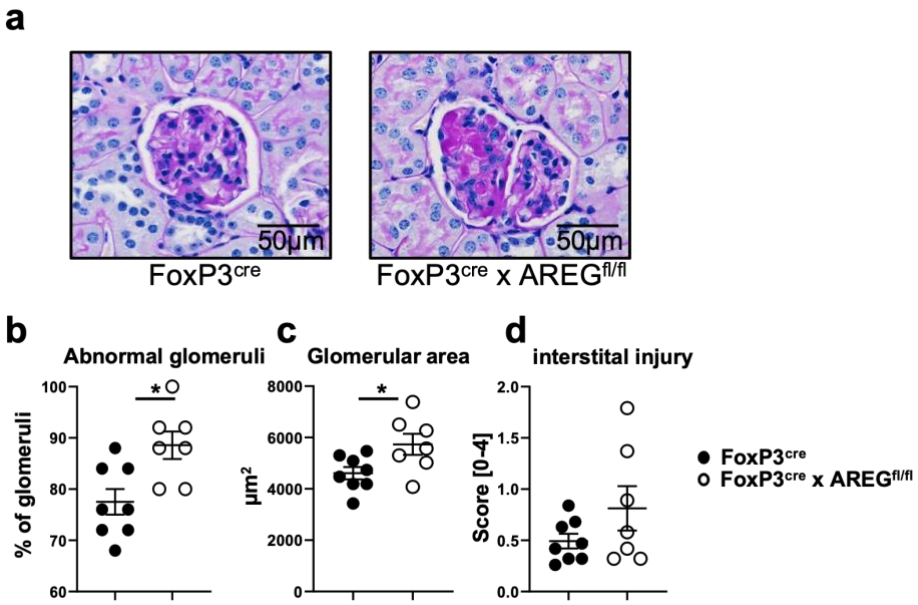

Figure 8: Deficiency of AREG in Tregs aggravates pristane-induced LN
(a) Representative PAS-stained kidney sections from the indicated mouse strains at 12 months of pristane-induced lupus nephritis (LN). (b-d) Quantification of (b) abnormal glomeruli, (c) glomerular area, (d) interstitial injury at 12 months after LN induction. Symbols show individual animals, horizontal lines show mean values. Error bars show the standard error of the mean. *p<0.05

Continuing my investigation, I sought to explore the long-term effects of AREG deficiency in Tregs by extending the disease period to 15 months after LN induction. In line with our 12-month data, also after 15 months, mice lacking AREG selectively in Tregs exhibited a significant increase in abnormal glomeruli and an enlarged glomerular area (Fig. 9a, b, c). Additionally, the interstitial injury was notably more severe in these mice (Fig. 9d).

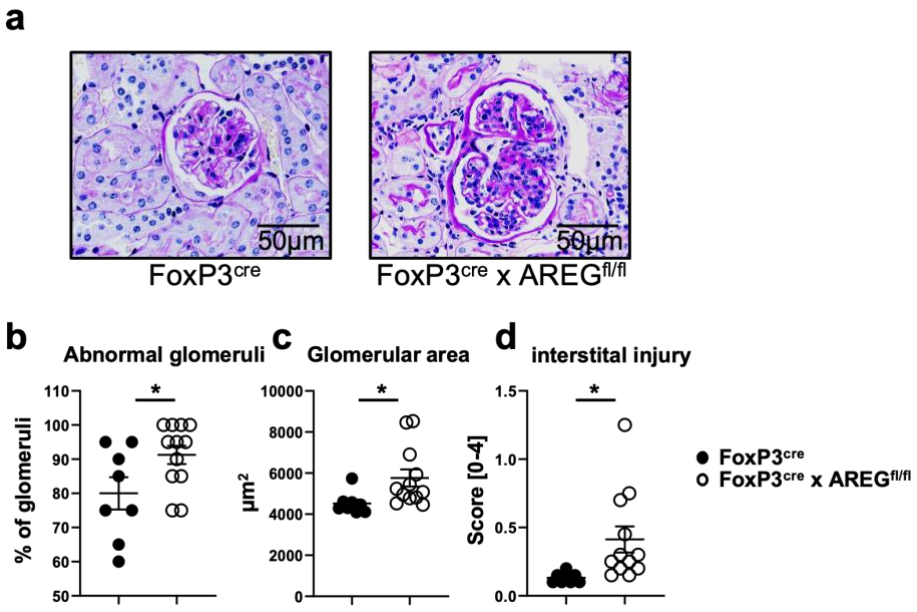

Figure 9: The protective effects from Treg-derived AREG are accentuated in the long-term

(a) Representative PAS-stained sections of kidneys from the indicated strains of mice at 15 months of pristane-induced lupus nephritis (LN). (b-d) Quantification of (b) abnormal glomeruli, (c) glomerular area, (d) interstitial injury at 15 months after LN induction. Symbols show individual animals, horizontal lines show mean values. Error bars show the standard error of the mean. *p<0.05.

These results suggest an enduring protective role of AREG derived from Tregs by mitigating the histological damage of the kidney in pristane-induced LN.

Next, I wanted to investigate if the observed protective effect of Treg-derived AREG is a result of an enhanced anti-inflammatory phenotype. Therefore, I in depths analyzed renal and systemic cellular and humoral immunity.

3.4. The absence of AREG derived from Tregs does not affect cellular immune responses

Considering the observation of increased kidney damage in FoxP3^{cre} x AREG$^{fl/fl}$ mice compared to WT mice, I hypothesized that this could be attributed to increased levels of pro-inflammatory cytokine secretion by CD4$^+$ T cells. This concept was particularly interesting, given our earlier findings, which demonstrated a potent anti-inflammatory AREG effect in pristane-induced LN via downregulation of CD4$^+$ T cell responses [126].

To investigate the influence of AREG's absence in Tregs on cellular immune responses I employed FACS staining to analyze immune cells from kidneys and

spleens of mice with pristane-induced LN. At 12 months after LN induction in FoxP3^{cre} x AREG$^{fl/fl}$ mice, Teff within the kidney did not exhibit significantly enhanced cytokine expression in comparison to AREG-sufficient controls. IFNγ secretion was even reduced (Fig. 10a). Moreover, the proliferation of Teffs, assessed through the expression of the proliferation marker Ki67 remained unaffected. Likewise, no significant difference in naïve, labeled as CD62L^{high} and CD44^{low} (Fig. 10b), or memory, labeled as CD62L^{low} and CD44^{high} (Fig. 10c) Teffs was detectable in the kidneys. Similarly, immune cells in the spleen did not demonstrate significant differences in their cytokine production, proliferation, or polarization (Fig. 10d-f).

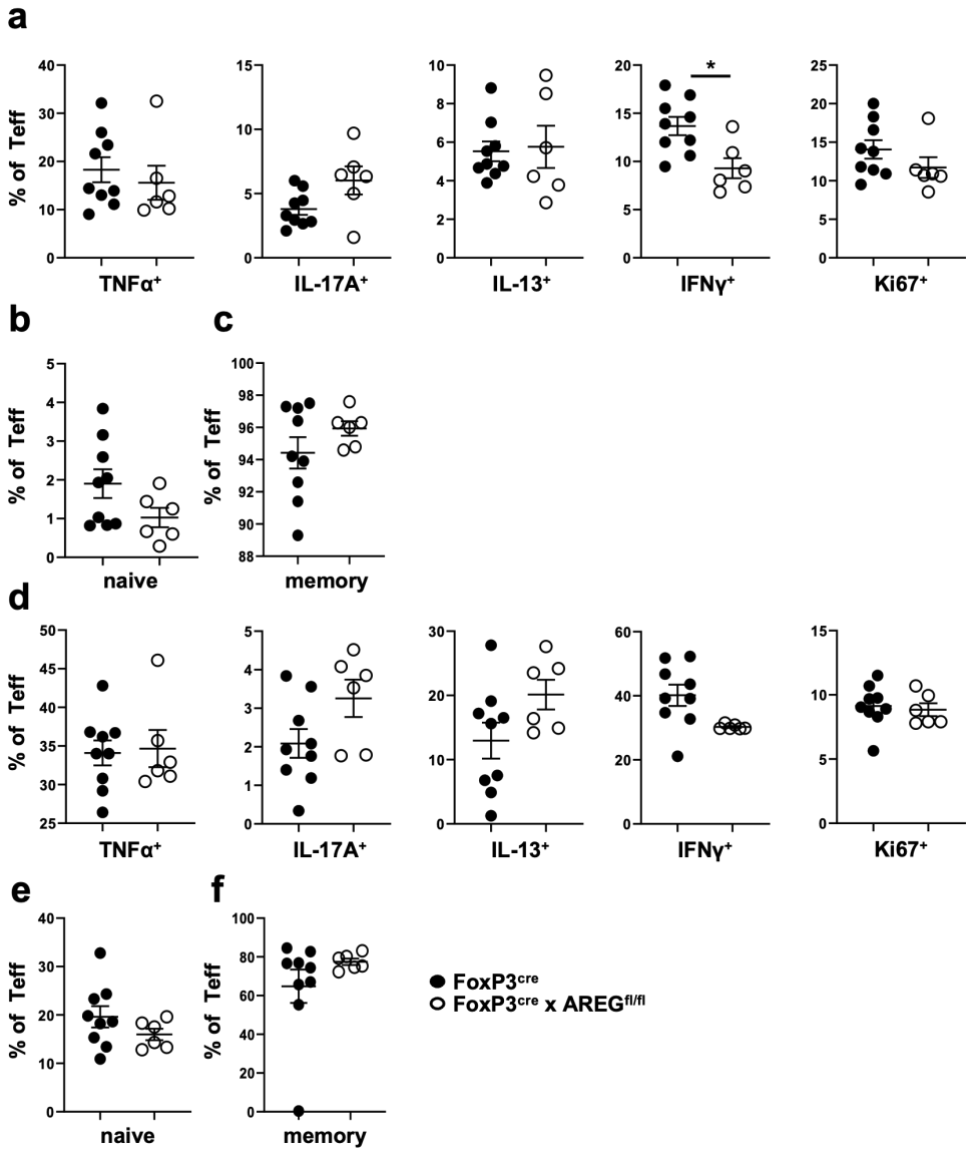

Figure 10: Lack of Treg-derived AREG does not affect CD4+ Teff responses at 12 months of LN

(a) Cytokine production (Tumor necrosis factor alpha (TNF-α), Interleukin 17A (IL-17A), Interleukin 13 (IL-13), Interferon-gamma (IFNγ)) and proliferation (Ki67) of effector T cells (Teffs) in Kidneys from mice of the indicated strains at 12 months of pristane-induced lupus nephritis (LN). (b) Naïve Teffs of kidneys from indicated mice labeled as $CD62L^{high}$, $CD44^{low}$. (c) Memory Teffs in kidneys from indicated mice labeled as $CD62L^{low}$, $CD44^{high}$. (d) Cytokine production and proliferation of Teffs from spleens of indicated strains at 12 months after induction of pristane-induced LN. (e) Naïve Teffs of spleens from indicated mouse strains labeled as $CD62L^{high}$, $CD44^{low}$. (f) Memory Teffs of spleens from indicated mouse strains labeled as $CD62L^{low}$, $CD44^{high}$. Symbols show individual animals and horizontal lines show mean values. Error bars show the standard error of the mean. *$p<0.05$.

Along the same line, following a 15-month duration of pristane-induced LN, no significant differences were observed in the levels of pro-inflammatory cytokines within the kidney (Fig. 11a) or spleen (Fig. 11b).

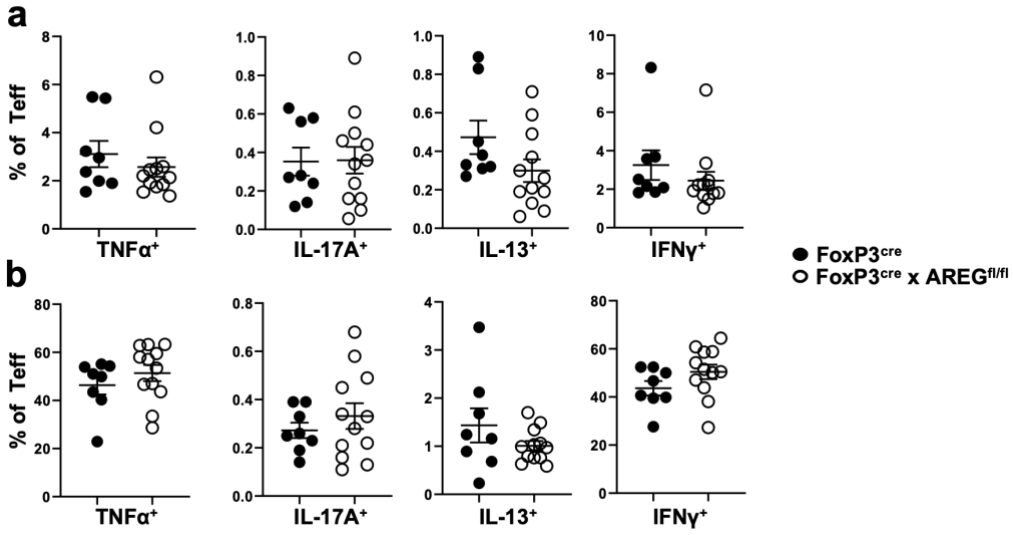

Figure 11: Lack of Treg-derived AREG does not affect CD4$^+$ Teff responses at 15 months of LN

Cytokine production (Tumor necrosis factor alpha (TNF-α), Interleukin 17 (IL-17), Interleukin 13 (IL-13), Interferon-gamma (IFNγ)) of effector T cells (Teffs) in kidneys (a) and spleens (b) of FoxP3^{cre} x AREG$^{fl/fl}$ mice or the respective controls at 15 months of pristane-induced lupus nephritis (LN). Symbols show individual animals and horizontal lines show mean values. Error bars show the standard error of the mean.

In summary, my data showed negligible effects of Treg-derived AREG on CD4$^+$ Teff responses. I therefore went on to study the effects on innate cells.

3.5. Deficiency of AREG in Tregs does not lead to alterations of macrophage phenotypes

In our previously published study, we demonstrated that AREG secreted by renal resident cells has strong effects on macrophages. AREG promoted the polarization of the pro-inflammatory M1 subtype and protected them from apoptosis in a mouse model of acute glomerulonephritis [131] as well as in pristane-induced LN [126]. In the present investigation, I therefore aimed to determine, whether AREG derived from Tregs would recapitulate this phenomenon or might even have other effects on the macrophage phenotype in the pristane-induced LN model. To identify macrophages, I performed cell gating and subsequently stained the cells for Ly6C, with a high expression indicating M1 polarization and a low expression indicating M2 polarization (Fig. 12a). However, the macrophages present in the kidneys of nephritic FoxP3^{cre} x AREG$^{fl/fl}$ mice displayed no significant differences in their polarization. To assess macrophage apoptosis and proliferation, we isolated

macrophages from the peritoneum of pristane-injected mice. Subsequent staining with annexin V and the proliferation maker Ki67 did not reveal any noticeable differences in macrophage apoptosis (Fig. 12b) or proliferation (Fig. 12c) when AREG was absent in FoxP3$^+$ Tregs.

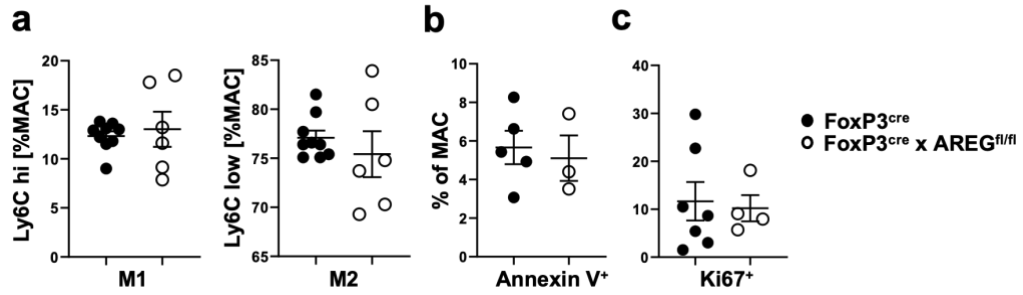

Figure 12: Lack of AREG in Tregs does not affect macrophage polarization, apoptosis, or proliferation

(a) FACS analysis of kidney macrophage (MAC) polarization into pro- (M1) and anti-inflammatory (M2) macrophages as assessed by expression of Ly6C in the indicated strains of mice after 12 months of pristane-induced lupus nephritis (LN). (b) Macrophage apoptosis as measured by annexin V staining of pristane-induced peritoneal macrophages in the indicated strains of mice. (c) Proliferation of macrophages as measured by Ki67 Staining of pristane-induced peritoneal macrophages in the indicated strains of mice. Symbols show individual animals, horizontal lines show mean values. Error bars show the standard error of the mean.

Contrary to our previously published data using pan-knockout AREG mice, my current findings present a contrasting result, indicating that the deficiency of AREG specifically in Tregs does not significantly impact the polarization, proliferation, or apoptosis of macrophages, as initially hypothesized.

Taken together, the above-described results clearly show, that Treg-derived AREG does not have relevant effects on CD4$^+$ T cell or macrophage activation and cytokine secretion. Therefore, another mechanism seems to be responsible for the observed protective effect of Treg-derived AREG in LN. One possibility would be AREG's effects on SLE characteristics humoral autoimmunity. Therefore, I went on to study this aspect.

3.6. Treg-derived AREG does not alter humoral lupus auto-immunity

My data show that cellular immune responses were not increased in FoxP3^{cre} x AREG$^{fl/fl}$ mice compared to the WT controls. Therefore, I checked for LN characteristic changes in the humoral immune response. The amount of plasma total IgG (Fig. 13a) showed no significant differences in the mice lacking AREG from

Tregs at 12 months after pristane-induced LN. The prototype LN marker plasma anti-dsDNA antibodies (Fig. 13b), as well as the anti-U1-snRNP antibodies (Fig. 13c), also remained unaffected by the absence of Treg-derived AREG.

Since our group recently showed, that the complete absence of AREG leads to increased glomerular C3 and IgG deposition in the kidney [126], I also investigated this aspect in mice with Treg-restricted AREG deficiency at 12 months after LN induction. However, neither increased glomerular complement component 3 (C3) (Fig. 13d) nor mouse IgG (Fig. 13e) deposition was found.

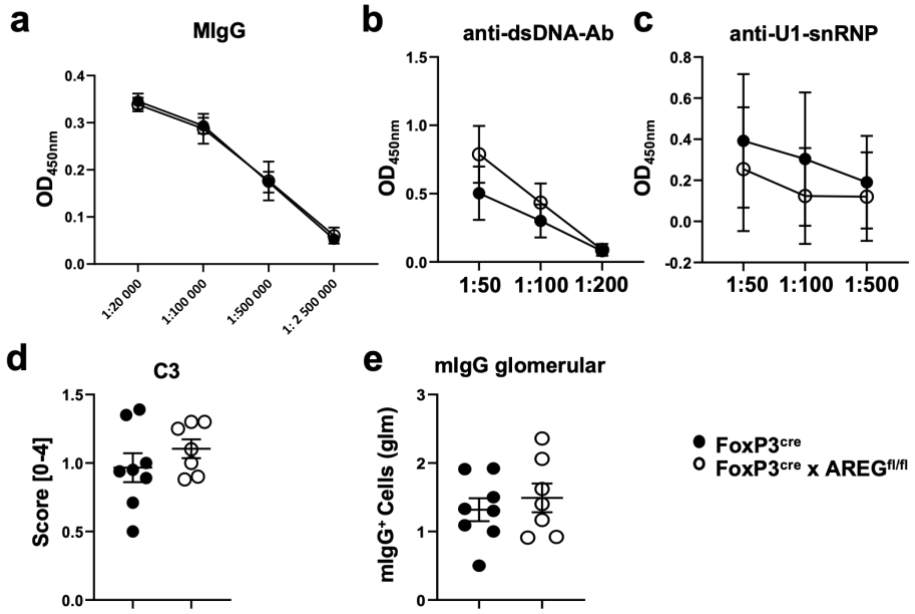

Figure 13: Lack of AREG from Tregs does not affect humoral immune responses
(a-c) Plasma-analysis of (a) total mouse IgG (m IgG) (b) anti-dsDNA antibodies (c) anti-U1-snRNP antibodies at 12 months of pristane-induced lupus nephritis LN in the indicated strains of mice at the indicated dilutions (d-e) Quantification of (d) complement component 3 (C3) and (e) mIgG deposition in glomeruli (glm) at 12 months of pristane-induced LN in the indicated strains of mice. OD: optical density. Symbols in a-c show mean values and bars show SEM. Symbols in (d) + (e) show individual animals and horizontal lines show mean values. Error bars show the standard error of the mean.

Also in the long run, after 15 months of pristane-induced LN, I could not see any differences in plasma total IgG (Fig. 14a), anti-ds-DNA-Ab (Fig. 14b), or anti-U1-snRNP antibodies (Fig. 14c). Similarly, selective AREG deficiency in Tregs did not have an impact on the LN characteristic glomerular C3 (Fig. 14d) or IgG (Fig. 14e) deposition at 15 months of pristane-induced LN.

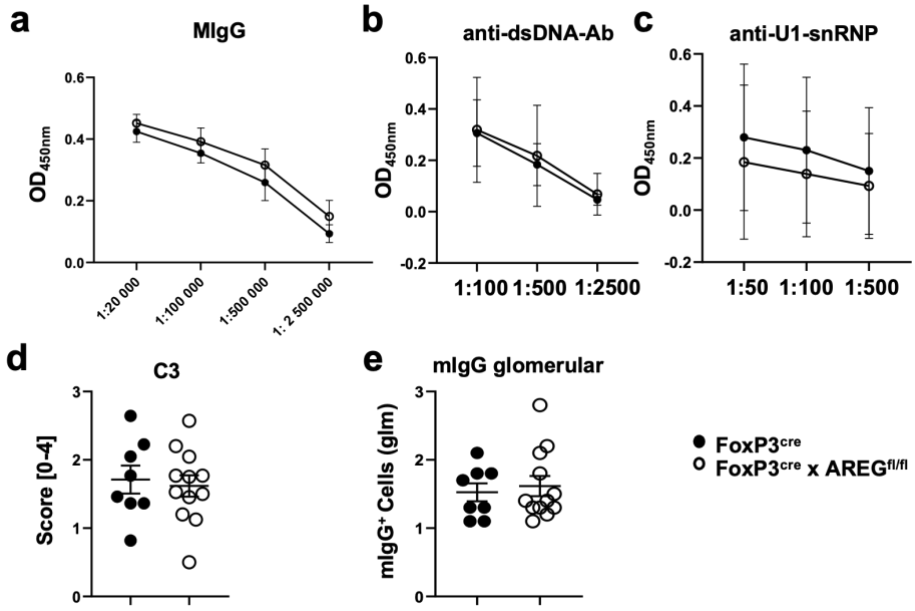

Figure 14: Long-term deficiency of AREG from Tregs does not affect humoral immune responses

(a-c) Plasma analysis of (a) total mouse IgG (mIgG) (b) anti-dsDNA antibodies (c) anti-U1-snRNP antibodies at 15 months of pristane-induced lupus nephritis (LN) in the indicated strains of mice at the indicated dilutions (d-e) Quantification of (d) complement component 3 (C3) and (e) mIgG deposition in glomeruli (glm) at 15 months of pristane-induced LN in the indicated strains of mice. OD: optical density. Symbols in a-c show mean values and bars show the standard error of the mean. Symbols in (d) + (e) show individual animals and horizontal lines show mean values. Error bars show the standard error of the mean.

At this point, it seemed unlikely, that Treg-derived AREG mediates protective effects via immunomodulation. This led me to the question of whether there are other, non-immune cell-mediated mechanisms affected by Treg-derived AREG.

3.7. Treg-derived AREG ameliorates fibrosis and apoptosis

It has recently become clear, that AREG is an important player in the balance between tissue repair and fibrosis. I, therefore, aimed to investigate the tissue-reparative effects of Treg-derived AREG in LN.

Indeed, kidneys of FoxP3^{cre} x AREG$^{fl/fl}$ mice at 12 months after pristane-induced LN demonstrated significantly increased fibrosis (Fig. 15a, b). I was also able to show, that age-matched naïve mice showed no increased fibrosis in comparison to FoxP3^{cre} x AREG$^{fl/fl}$ mice at 12 months after pristane-induced LN. Consistent with these findings, fibrotic changes of interstitial kidney tissue remained aggravated compared to the control group also after 15 months (Fig. 15c, d).

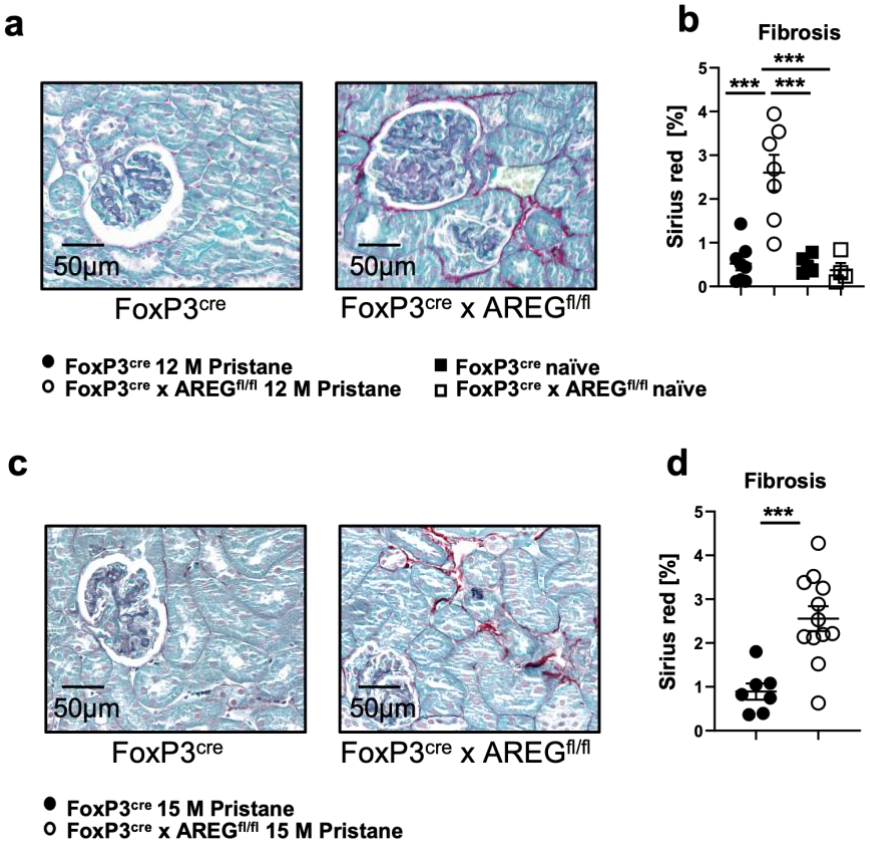

Figure 15: Treg-derived AREG ameliorates renal fibrosis

(a) Representative Sirius Red stained sections of Kidneys from FoxP3^{cre} controls and FoxP3^{cre} x AREG$^{fl/fl}$ mice at 12 months of pristane-induced lupus nephritis (LN). (b) Quantification of fibrosis at 12 months after LN induction as well as age-matched naïve FoxP3^{cre} controls and FoxP3^{cre} x AREG$^{fl/fl}$ mice. (c) Representative Sirius Red stained sections of Kidneys from FoxP3^{cre} and FoxP3^{cre} x AREG$^{fl/fl}$ mice at 15 months of pristane-induced LN. (d) Quantification of fibrosis at 15 months after LN induction. Symbols show individual animals and horizontal lines show mean values. Error bars show the Standard error of the mean. *** $p<0.001$

Another characteristic change found in LN is increased apoptosis of renal resident cells. I, therefore, wanted to investigate the potential effects of Treg-derived AREG on caspase 3 expressing cells in renal tissue. Indeed, after 15 months of pristane-induced LN, increased numbers of apoptotic cells were observed in kidney sections of FoxP3^{cre} x AREG$^{fl/fl}$ mice (Fig. 16a, b).

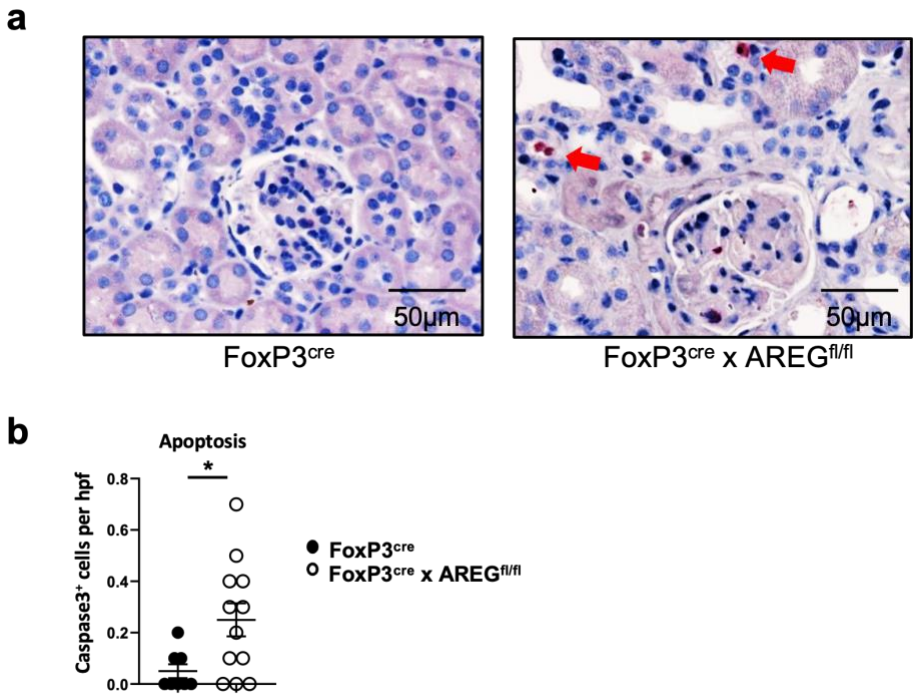

Figure 16: Lack of AREG derived from Tregs leads to increased apoptosis
(a) Representative pictures of caspase 3 stained sections of kidneys from FoxP3^{cre} controls and FoxP3^{cre} x AREG$^{fl/fl}$ mice at 15 months of pristane-induced lupus nephriris (LN). (b) Quantification of caspase 3 positive cells per high power field (hpf) at 15 months after LN induction. Symbols show individual animals and horizontal lines show mean values. Error bars show the standard error of the mean. * $p<0.05$

Taken together, the above findings suggest a long-term protective role of Treg-derived AREG in LN by mitigating histological damage as well as protection against apoptosis and renal fibrosis. This effect is not visible in healthy age-matched mice Interestingly, these alterations seem to be independent of any effects on nephritogenic immune responses.

Next, I wanted to investigate if the observed protective effects are limited to Treg-derived AREG or if AREG secreted by other immune cells might exert similar functions.

3.8. Macrophage-derived AREG did not alter the renal outcome or fibrosis in pristane-induced LN

In addition to Treg-derived AREG, AREG secreted by macrophages has also been described as having potent tissue-protective effects. Furthermore, our results from human LN, shown above, confirmed macrophages as a major source of renal AREG

expression. In order to follow up on this notion, we generated LysM^{cre} x AREG$^{fl/fl}$ mice, in which AREG production is abolished in most myeloid cell lineages, including monocytes and macrophages. These mice were induced with pristane LN and renal damage was assessed after 12 months. Intriguingly, I did not observe any significant differences in renal damage between mice lacking AREG production in myeloid cells and control mice (Fig. 17a, b).

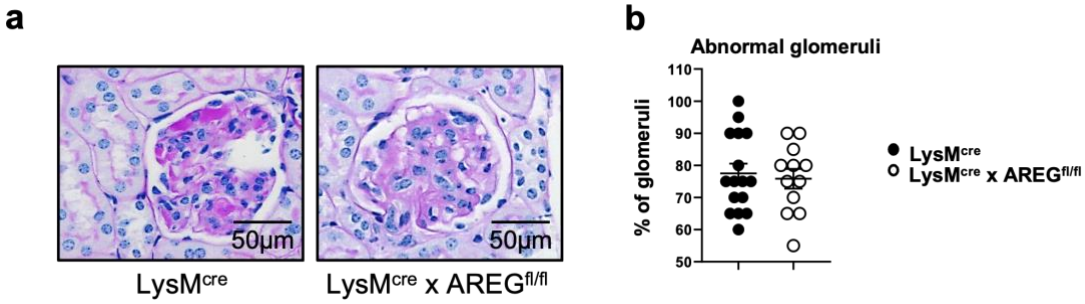

Figure 17: Macrophage-derived AREG does not affect the outcome of LN
(a) Representative PAS-stained sections of kidneys from the indicated strains of mice at 12 months of pristane-induced lupus nephritis (LN) (b) Quantification of abnormal glomeruli in kidneys of LysM^{cre} x AREG$^{fl/fl}$ and control mice at 12 months of pristane-induced LN. Symbols show individual animals and horizontal lines show mean values. Error bars show the standard error of the mean.

Similarly, examination of renal fibrosis revealed no significant difference between the two groups (Fig. 18a, b). These findings highlight the cell type-specific effects of AREG coming from Tregs.

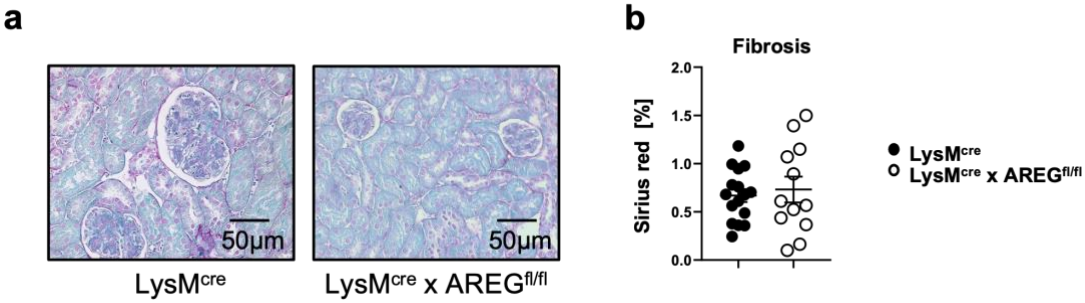

Figure 18: Lack of AREG in macrophages does not alter renal fibrosis
(a) Representative Sirius red-stained sections of kidneys from the indicated strains of mice at 12 months of pristane-induced lupus nephritis (LN). (b) Quantification of fibrosis in kidneys of LysM^{cre} x AREG$^{fl/fl}$ and control mice at 12 months of pristane-induced LN. Symbols show individual animals and horizontal lines show mean values. Error bars show the standard error of the mean.

Furthermore, I investigated the potential immunological phenotypes associated with the loss of AREG from myeloid cells. Similarly, to the situation in mice with loss of

Treg-derived AREG, cytokine production from Teffs exhibited no significant difference in kidneys (Fig. 19a) and spleens (Fig. 19c). Interestingly, and in line with our previous study, I observed a decrease in M1 and an increase in M2 polarization in macrophages from mice lacking AREG production from myeloid cells (Fig. 19b).

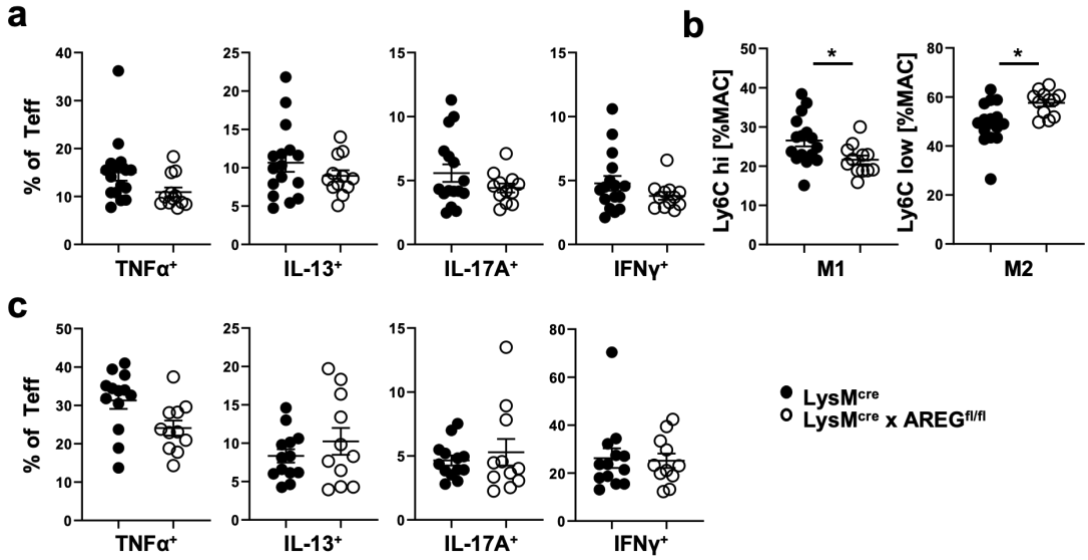

Figure 19: Effects of macrophage-derived AREG on cellular immune responses in LN

(a) Cytokine Expression (Tumor necrosis factor alpha (TNF-α), Interleukin 17 (IL-17), Interleukin 13 (IL-13), Interferon-gamma (IFNγ)) by effector T cells (Teffs) in the kidney of $LysM^{cre}$ x $AREG^{fl/fl}$ mice or controls at 12 months of pristane-induced lupus nephritis (LN) (b) Kidney macrophage (MAC) polarization into pro- (M1) and anti-inflammatory (M2) phenotypes as measured by expression of Ly6C in the indicated strains of mice at 12 months after pristane injection (c) Cytokine expression by Teffs in the spleen of $LysM^{cre}$ x $AREG^{fl/fl}$ mice or controls at 12 months of pristane induced LN. Symbols show individual animals and horizontal lines show mean values. Error bars show the standard error of the mean. *$p<0.05$.

Collectively, my data demonstrate, that the tissue-protective effects of AREG are specifically mediated by AREG derived from Tregs. Conversely, the absence of AREG production in macrophages primarily promotes polarization toward anti-inflammatory M2 Macrophages without discernible impact on fibrosis and the overall renal outcome in LN.

I thus aimed to investigate the so far unclear mechanisms underlying the observed reno-protective effects of Treg-derived AREG.

3.9. The addition of recombinant AREG leads to improved wound healing in vitro

My above-outlined data highlight the significance of AREG from Tregs in protecting against renal damage and consecutive fibrosis in LN. To investigate, whether these effects are mediated via the direct roles of AREG on tissue repair, murine mesangial cells (mMC) and murine tubulous cells (mTC) were used in an *in vitro* scratch assay to assess wound healing. Interestingly, both mMC (Fig. 20a, b) and mTC (Fig. 20c, d) exhibited significantly improved wound healing in the presence of recombinant AREG compared to the control condition.

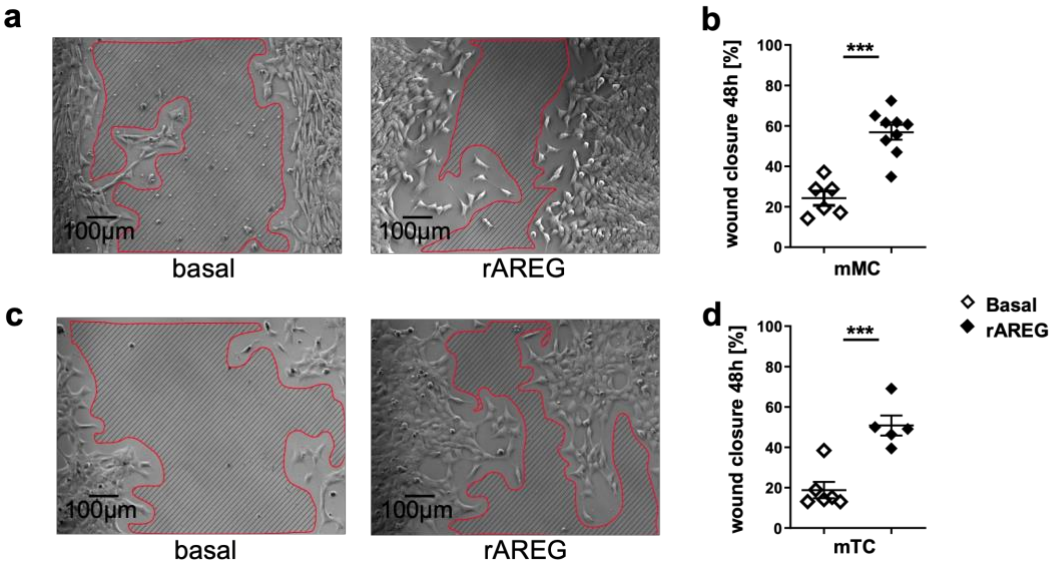

Figure 20: The addition of recombinant AREG leads to improved wound healing
(a) Representative pictures of wound closure at 48 h after application of a scratch to a layer of murine mesangium cells (mMC) with or without recombinant AREG (rAREG) (b) Quantification of wound closure at 48 h after application of a scratch to a layer of mMC with or without rAREG (c) Representative pictures of wound closure at 48 h after application of a scratch to a layer of murine tubulous cells (mTC) with or without rAREG. (d) Quantification of wound closure at 48h after application of a scratch to a layer of mTC with or without rAREG. Symbols represent independent biological replicates and horizontal lines show mean values. Error bars show the standard error of the mean. ***$p<0.001$

After having shown the effects of AREG on mesenchymal and epithelial cells, I next aimed to analyze effects on endothelial cells, in particular since AREG has been reported to demonstrate positive effects on restoration of vascularization [115]. I, therefore, obtained human glomerular endothelial cells (hGEnC), considering the pivotal role of this cell type in the glomerular healing processes. Similar to the results

using mMC and mTC, a scratch assay showed increased wound healing at 8 h in the presence of recombinant AREG (Fig. 21a, b).

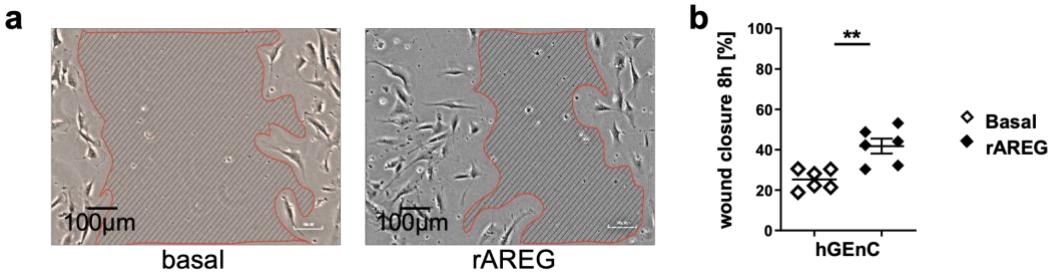

Figure 21: Improved wound healing in human glomerular endothelial cells after the addition of rAREG

(a) Representative pictures of wound closure at 8 h after application of a scratch to a layer of human glomerular endothelial cells (hGEnC) with or without recombinant AREG (rAREG). (b) Quantification of wound closure at 8 h after application of a scratch to a layer of hGEnC with or without the addition of recombinant AREG. Symbols represent independent biological replicates and horizontal lines show mean values. Error bars show the standard error of the mean. **$p<0.01$,

In summary, across diverse cell types from mice and humans, including mMC, mTC, and hGEnCs the scratch assay demonstrates accelerated wound healing in the presence of recombinant AREG. This underscores the potential applicability of therapeutic AREG in promoting reparative processes across different cellular contexts.

Additionally, we explored the effects of AREG on the growth and tube formation of hGEnC. This investigation involved a tube formation assay, wherein the endothelial cells were seeded on matrigel, a substrate promoting the formation of 3D structures like capillaries. Subsequently, these structures were quantified using an analysis tool within ImageJ. The tool identified 1) junctions represented as a group of adjacent dots, grouped into master junctions (yellow), and 2) extremities, depicted as pixels with only one neighboring pixel. In subsequent analyses, the tool assessed 1) branches (shown in green lines) defined as lines linked to one junction and forming one extremity, 2) segments (shown by magenta circles) defined as lines connected to the main tree by two junctions, and 3) meshes (shown in light blue) defined as enclosed areas. Isolated elements are shown in dark blue [144]. The result of this analysis is shown as a representative picture in Figure 22a. Recombinant AREG notably facilitated the total branches' length after 30 h (Fig. 22b) the number of branches (Fig. 22c), the number of segments (Fig. 22d), and the number of meshes (Fig. 22e)

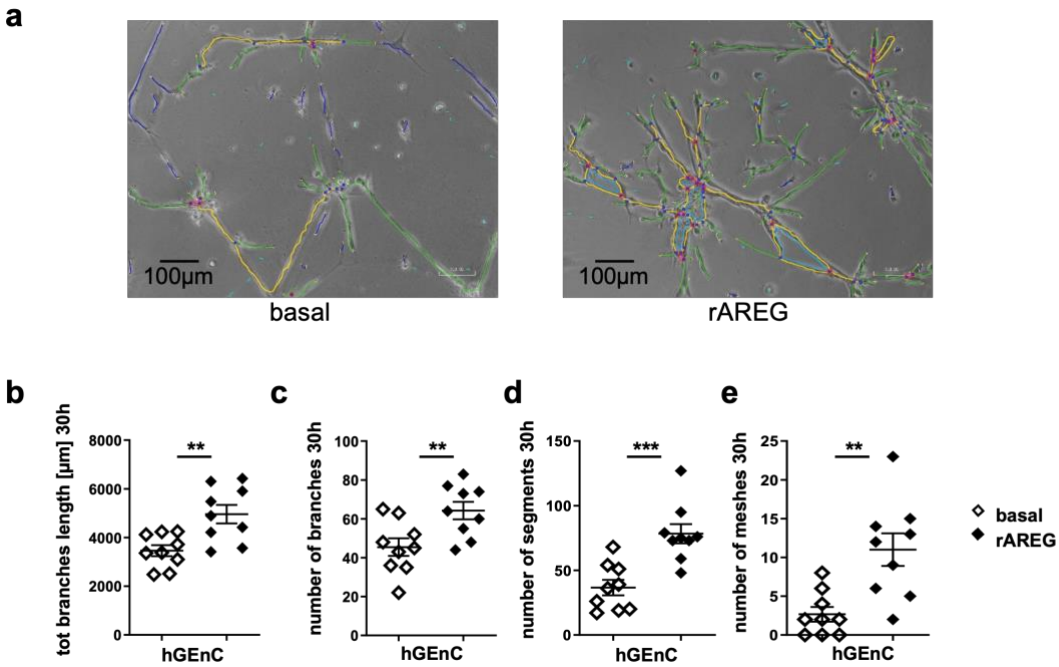

Figure 22: AREG enhances the growth of renal microvasculature

(a) Representative pictures of tube formation assays of hGEnC with or without the addition of recombinant AREG (rAREG) after 30 h. Branches are shown in green, segments are shown in magenta, and meshes are shown in light blue. (b) Quantification of total branches length (c) number of branches, (d) number of segments, and (e) number of meshes. Symbols represent individual cell culture preparations; horizontal lines show mean values. Error bars show the standard error of the mean. **p<0.01, ***p<0.001

In summary, the addition of AREG increased the number and length of branches, as well as the number of segments, and meshes.

In conclusion, my investigation reveals that the addition of recombinant AREG not only enhances cell migration and wound healing across various cell types but also amplifies growth and tube formation in hGEnCs. These findings underscore the potential therapeutic relevance of AREG in promoting tissue repair and angiogenesis in the context of diverse cellular environments.

4. Discussion

Despite significant research, LN remains a major cause of morbidity and mortality in the SLE population. Existing treatment options often fail to induce disease remission, and patients may develop ESKD within only a decade [14]–[16]. Understanding LN pathophysiology is crucial for developing targeted and effective treatment strategies. LN is characterized by pathological type I interferon signaling, impaired cellular apoptosis, and dysregulated immune responses, leading to the activation of various immune cells and the emergence of autoantibodies against nuclear components [17]–[26].

The dysregulation of immune responses in LN involves the activation of diverse autoreactive T-cell subtypes by dendritic cells. T follicular helper cells stimulate B cells to produce nephritogenic autoantibodies, Th1 cells contribute to IFN-γ production which activates tissue destructive macrophages, and Th17 cells induce kidney injury by activating neutrophils. Tregs play a crucial role in counterbalancing these autoreactive lymphocytes, suppressing both B- and T-cell activity [11], [26]-[28]

This complex interplay of immune cells and the dysregulated immune response in LN lays the foundation for a discussion regarding potential therapeutic interventions and future research directions. One promising target could be the EGFR signaling cascade.

The EGFR and its ligands, play crucial roles in kidney biology, influencing regeneration, fibrosis, and immune responses [102]–[106]. AREG, one of the EGFR ligands, is known for mediating tissue repair as well as anti-inflammatory effects like enhancing the suppressive capacity of Tregs [126]. However, AREG showcases a dual and contradictory role by also initiating pro-inflammatory macrophage activation, thus mediating additional and context-dependent disease-aggravating effects [133].

Beyond immunomodulation, AREG's Janus-faced nature also extends to fibrosis. While well recognized for tissue reparative functions (reviewed in [100]), AREG can also contribute to fibrosis in specific contexts, leading to loss of function in various organs, including the kidneys [101], [133]–[137]. Interestingly, the cellular source of AREG seems to be of major importance for its functional role. While AREG coming from leukocytes like Tregs, ILC2s, γδT cells, mast cells, basophils, and

monocytes/macrophages was shown to be anti-inflammatory and tissue-protective [116], [121], [124], [145]–[147], AREG secreted by tissue-resident cells is pro-inflammatory and disease aggravating [131].

Interpreting the complex roles of AREG coming from different cellular sources is thus pivotal for understanding its potential as a therapeutic target in the broad landscape of renal diseases.

With this thesis I am particularly investigating the role of Treg-derived AREG in LN, trying to figure out its importance and mechanisms of action with the final goal of evaluating AREG´s suitability as a potential therapeutic target.

4.1. AREG in human lupus nephritis

In our recent study, we identified a sum protective role of AREG against experimental LN by broadly attenuating pathogenic $CD4^+$ Teff responses. This discovery further gained importance by our finding of strong AREG upregulation in renal biopsies from patients with LN. Our comprehensive analysis shown in Figure 5 utilized multiplexed immunohistochemistry to identify the leucocyte sources contributing to AREG expression. Notably, the quantitative valuation revealed $FoxP3^+CD4^+$ Tregs as well as $CD68^+$ monocytes/macrophages as the most abundant AREG-producing populations. Our results are in line with previously published studies in murine models. Macrophages were shown to be the critical source of AREG after tissue injury [116]. However, not only macrophages but also Tregs showed increased AREG expression in experimental mouse models [119].

In light of these findings, we aimed to look deeper into the specific contributions of AREG derived from Tregs and macrophages, employing a mouse model of LN as well as conditional knockout mice with Treg and monocyte/macrophage restricted AREG deficiency.

4.2. Treg restricted AREG knockout

Our previous investigation into the role of AREG in the pristane-induced LN mouse model has uncovered a crucial aspect of AREG's immunomodulatory function. The pan knockout of AREG resulted in an aggravated inflammatory response, emphasizing the immune-regulatory role of AREG in LN. One key mechanistic finding from our study is the direct downregulation of pathogenic Teff activation and cytokine production by AREG/EGFR signaling [126]. This finding aligns with

previous studies highlighting AREG's diverse roles in immune regulation. Notably, in line with data from other researchers, our analyses demonstrated that AREG can be produced by various cellular sources, both in the murine experimental model and in human LN. To further analyze the cell type-specific impact of AREG in LN, I focused first on the most prominent AREG-producing cell type in human Lupus nephritis, namely Tregs. By generating mice with Treg-restricted AREG deficiency (FoxP3^{cre} x AREG$^{fl/fl}$), I aimed to reveal the specific role of Treg-derived AREG in LN.

PCR analyses confirmed the successful excision of AREG coding DNA, specifically in the Tregs of these mice. Importantly, this AREG deficiency was not observed in other leukocyte subtypes nor non-lymphoid tissues, confirming the specificity of our genetic manipulation. Protein expression analysis via FACS analysis further supported these findings, demonstrating nearly absent AREG expression in Tregs from FoxP3^{cre} x AREG$^{fl/fl}$ mice in both the spleen and kidney.

These results establish FoxP3^{cre} x AREG$^{fl/fl}$ mice as a valuable tool for investigating the exclusive role of Treg-derived AREG in LN.

4.3. Treg-derived AREG protects from kidney damage in pristane-induced LN

After successfully establishing mice lacking AREG production from Tregs, I focused on unraveling AREG´s role in LN. Therefore, I used the pristane-induced LN mouse model and examined the damage to the kidney via histology analysis after 12 months. Our results revealed an exacerbation of LN in FoxP3^{cre} x AREG$^{fl/fl}$ mice compared to FoxP3^{cre} controls. This aggravation was evidenced by a significant increase in histologically abnormal glomeruli and an enlarged glomerular area in mice lacking AREG in Tregs.

Extending the disease period to 15 months reinforced our 12-month findings, demonstrating a persistent increase in abnormal glomeruli with enlarged glomerular area. At this later time point, we even found aggravated interstitial damage in mice lacking AREG selectively in Tregs.

These results strongly suggest a persistent protective role of Treg-derived AREG in mitigating histological kidney damage in pristane-induced LN.

These results align with our previously published data showing a protective role of AREG in LN [126]. Since our study had identified a strong immunomodulatory effect of AREG, in particular by downregulation of pro-inflammatory Teffs, we

wanted to explore, whether this mechanism would also underlie the reno-protective effects of Treg-derived AREG.

4.4. Treg-derived AREG has no impact on T cell responses

The observation of increased kidney damage in FoxP3^{cre} x AREG$^{fl/fl}$ mice prompted me to investigate the mechanisms underlying this phenomenon. Considering our prior findings highlighting the potent anti-inflammatory role of AREG in pristane-induced LN through the downregulation of cellular immune responses, it was a logical consequence to explore this notion.

However, contrary to this hypothesis, the absence of AREG in Tregs did not lead to a significant increase in pro-inflammatory cytokine secretion by CD4$^+$ T cells in the kidneys or spleens at 12 months after induction of LN. Surprisingly, IFN-γ secretion was even somewhat reduced. Further analysis of Teff proliferation and polarization also revealed no significant differences between AREG-deficient and AREG-sufficient controls, both in the kidneys and spleen.

This finding persisted even after extending the duration of pristane-induced LN to 15 months, indicating no relevant impact on CD4$^+$ Teff responses by Treg-derived AREG. These results clearly suggested that the increased kidney damage observed in FoxP3^{cre} x AREG$^{fl/fl}$ mice cannot be attributed to changes in CD4$^+$ Teff responses. Considering these findings, the focus shifted towards investigating the effects of Treg-derived AREG on innate immune cells, since we had previously reported a strong impact of AREG on macrophage polarization and activation [131].

4.5. No effects of Treg-derived AREG on the macrophage phenotype

My investigation next aimed to elucidate the specific impact of AREG derived from Tregs on macrophage dynamics within the context of pristane-induced LN. While our prior findings demonstrated potent effects of AREG on promoting pro-inflammatory M1 polarization and protecting them from apoptosis [131], the present study, focusing specifically on Treg-derived AREG, revealed a contrasting outcome. I assessed macrophage polarization in nephritic FoxP3^{cre} x AREG$^{fl/fl}$ mice but did not observe any significant differences in M1 or M2 polarization in macrophages isolated from the kidneys of these mice. Additionally, examinations of macrophage apoptosis and proliferation, critical indicators of their functional dynamics, did not show noticeable differences when AREG was absent in FoxP3$^+$ Tregs. These

findings contrast with our earlier research using pan-knockout AREG mice, which showed that AREG secreted by resident kidney cells induces polarization and proliferation of M1 Macrophages [131]. Also, other groups have previously described, that AREG can induce macrophage recruitment [148]. Furthermore, a separate investigation demonstrated an anti-inflammatory effect of AREG on macrophage polarization by showing that the in vitro reconstitution with recombinant AREG can revert the polarization of macrophages from M1 back to M2 [149]. It is important to mention again that these two studies did not investigate the specific function of Treg-derived AREG. Taken together, my data indicate, that Treg-derived AREG doesn't have a relevant impact on cellular immunity and protects from LN via other mechanisms.

4.6. AREG from Tregs does not alter humoral lupus immunity

Similar to our results from cellular immune responses, analysis of humoral immunity in FoxP3^{cre} x AREG$^{fl/fl}$ mice did not reveal significant changes in comparison to the WT control. Despite the deficiency of AREG in Tregs, there were no noticeable changes in serum total IgG levels, anti-dsDNA, or anti-U1-snRNP antibodies at both 12 and 15 months of pristane-induced LN. Along the same line, in the kidneys of nephritic mice with Treg-specific AREG deficiency, there were no noticeable differences in glomerular C3 or mIgG deposition. Together, these data suggest, that Treg-derived AREG does not play a significant immunomodulatory role in the context of LN. This raises the possibility that the protective effects of Treg-derived AREG most likely involve non-immune-cell mediated mechanisms.

4.7. Treg-derived AREG ameliorates kidney fibrosis

After figuring out, that Treg-derived AREG protects from kidney damage in pristane-induced LN and that this is independent of the immune system, my investigation focused on non-immune mechanisms. The examination of kidneys from FoxP3^{cre} x AREG$^{fl/fl}$ mice, at 12 months of pristane-induced LN, revealed a noteworthy increase in renal fibrosis compared to their control counterparts. This difference was not visible in naïve age-matched control mice of these two strains. Hence, the reno-protective effect of Treg-derived AREG relies on the context of LN. The increased degree of fibrosis persisted even at the 15-month time point, emphasizing the enduring impact of Treg-derived AREG on tissue injury in

inflammatory kidney disease. In addition to increased fibrosis, we also found a substantial increase in renal apoptotic cells after 15 months of pristane-induced LN in FoxP3^{cre} x AREG$^{fl/fl}$ mice. Collectively, these findings show the long-term protective role of Treg-derived AREG in mitigating histological damage by decreasing apoptosis and attenuating renal fibrosis.

Supporting our findings, several previous studies provided evidence of AREG upregulation in various models of organ fibrosis, suggesting its functional involvement in fibrotic processes [135], [150]–[152].

Three of these studies specifically dealt with the role of AREG in kidney fibrosis. In contrast to our observations, all of them consistently demonstrated a pro-fibrotic role of AREG [137], [151], [152]. This discrepancy in outcomes between my study and the aforementioned studies may be attributed to the critical factor of cell type-specific differential roles of AREG. In my case, I investigated the specific role of AREG produced by Tregs, while the three other studies either completely neutralized AREG, regardless of its source, or focused on proximal tubule-derived AREG. Importantly, those studies found pro-inflammatory effects of AREG, in particular activation of pro-fibrotic macrophages and/or renal CCL2/MCP-1 and TNFα overexpression. Therefore, it is highly likely, that the observed aggravation of fibrosis in the presence of AREG is secondary to increased inflammation rather than a direct AREG-induced effect. In my study of LN, in contrast, lack of Treg-derived AREG did not result in any measurable effects on immunity, so the observed amelioration of renal fibrosis is rather a direct AREG-mediated effect. These findings again emphasize that the cellular source of AREG is indeed crucial for its function, regardless of whether AREG is genetically silenced, interrupted by RNA interference, or neutralized by antibodies.

However, to make things even more complicated, another recent study failed to detect significant differences in liver fibrosis using the same FoxP3^{cre} x AREG$^{fl/fl}$ mice, as I did in our study [150]. This outcome, which contrasts with our findings, might be attributed to the relatively short duration of the model, which lasted no longer than 8 weeks. The function of AREG thus does not only seem to depend on the cellular source but also on the experimental context, in particular the time axis as well as the organ of damage.

4.8. Renal tissue protection in LN is a specific feature of Treg-derived AREG

The intricate interplay between tissue repair and fibrosis involves complex molecular mechanisms, and recent attention has focused on AREG as a key player in this balance. In my study, I observed a reduction of renal cell apoptosis and renal fibrosis in the presence of Treg-derived AREG. Next, I aimed to clarify, whether this is indeed a cell type-dependent AREG function or if AREG from other sources also elicits the same effects. In addition to Treg-derived AREG, macrophage-secreted AREG has been recognized for its potent tissue-protective effects [116]. Our results from analyses of human LN biopsies could verify macrophages as a significant source of renal AREG expression. To understand the specific effects of macrophage-secreted AREG, $LysM^{cre}$ x $AREG^{fl/fl}$ mice were generated to eliminate AREG production in myeloid cell lineages, including monocytes and macrophages. However, in contrast to mice lacking Treg-derived AREG, no significant differences in renal damage or fibrosis were observed between mice lacking AREG in myeloid cells and control mice after 12 months of pristane-induced LN. This once more highlights the cell type-specific character of AREG´s effects and emphasizes the crucial role of Treg-derived AREG in renal protection.

The analysis of immunological phenotypes associated with the loss of AREG in myeloid cells revealed no significant difference in Teff cytokine production, aligning with findings in mice lacking Treg-derived AREG. Interestingly, consistent with our previous study, an increase in M2 polarization in macrophages from mice lacking AREG production by myeloid cells was observed [131]. However, this shift in macrophage polarization did not translate into evident impacts on renal outcomes or fibrosis in LN. These results collectively indicate that the tissue-protective effects of AREG are specifically mediated by AREG derived from Tregs. Conversely, the absence of AREG production in macrophages promotes polarization toward an anti-inflammatory M2 phenotype, while Treg-derived AREG does not have an impact on myeloid cell polarization. My data are in line with previously published observations. One study showed that bone-marrow-derived macrophages lacking AREG had decreased migration, reduced activation of pro-inflammatory genes associated with M1 polarization, and increased expression of anti-inflammatory genes associated with M2 polarization [153].

Concerning macrophage-derived AREG, however, different from our findings, several authors have described relevant tissue-protective effects in organs other than

the kidneys. A landmark study revealed that macrophage-derived AREG acts on pericytes to induce their differentiation into myofibroblasts, which promotes vascular wound healing after acute lung injury by nematode infection [116]. It is noteworthy, however, that AREG effects only became relevant in the recovery phase after the acute pulmonary infection. The pristane-induced LN, which was studied in my thesis, is a model of chronically progressive immune-mediated damage and therefore does not have a recovery phase like an infection with a nematode. In the acute infection phase with the nematode, also no relevant effects of macrophage-derived AREG were observed [116]. Therefore, while resident tissue cell-derived AREG acts during acute inflammation, Treg-derived AREG appears to exert its effects during chronic inflammatory processes and macrophage-derived AREG seems to fully unfold its effects only after cessation of inflammation during the recovery phase. Two further studies hypothesized, that AREG derived from macrophages seems to have a protective role in the context of experimental cardiac stress by pressure overload [117], [154]. Protection by macrophage-derived AREG included induction of cardiomyocyte hypertrophy as well as stabilization of inter-cardiomyocyte gap junctions. Since the affected cells and pathways are heart-specific, those results are difficult to compare to my study on kidney inflammation. Finally, one further study described a protective effect of macrophage-derived AREG in a model of autoimmune uveitis via both immune and non-immune mediated mechanisms. These findings, however, derive largely from in vitro neutralization of AREG in macrophage co-cultures and might thus not reflect the true in vivo situation [118].

4.9. Wound healing effects of AREG

The observed protective effects of AREG derived from Tregs in LN prompted an exploration of the underlying mechanisms. Given strong evidence from previous studies [120], [155], I particularly focused on AREG´s direct roles in tissue repair. As a model system, I chose an in vitro scratch assay. This served as a valuable tool to assess wound healing of cells from different renal compartments and different germinal sheets, including glomerular mesenchymal cells (murine mesangial cells, mMC), tubular epithelial cells (murine tubulus cells, mTC), and glomerular endothelial cells (human glomerular endothelial cells, hGEnC).

Notably, the application of recombinant AREG significantly improved wound healing in both, mMC and mTC, suggesting a direct influence of AREG on mesenchymal and epithelial cells. This effect also extended to hGEnCs. Therefore, the scratch assay demonstrated accelerated wound healing in the presence of recombinant AREG across diverse cell types from mice and humans. Also, other studies support my findings. One study showed that Treg-derived AREG enhances the growth and activation of lung alveolar mesenchymal cells during influenza virus infection [156].

Further exploration of AREG's impact on hGEnCs involved a tube formation assay, providing insights into its effects on angiogenesis. The analysis revealed that recombinant AREG significantly facilitated the growth and tube formation of hGEnCs, as evidenced by increased branches' length, number of branches, number of segments, and number of meshes. These findings are in line with previous observations by others and again highlight the pro-angiogenic properties of AREG. Interestingly, while previous studies have shown vascular repair effects via EGFR activation on pericytes as intermediaries [157], our data showed, that AREG can also directly act on vascular endothelial cells. Another group described a similar finding, using mouse aortic endothelial cells as well as human umbilical vein endothelial cells [117].

In conclusion, our investigation demonstrates that recombinant AREG not only enhances cell migration and wound healing in different cell types but also amplifies vascular growth and tube formation. These findings contribute valuable insights into the mechanisms through which Treg-derived AREG protects against renal damage and fibrosis in LN. Importantly, the consistent effects across different cell types and the promotion of angiogenic processes underscore the potential therapeutic relevance of AREG in the context of diverse cellular environments and diseases.

4.10. Amphi-Regulin: Discussing the dual regulatory protein

As research in recent years, including studies by our group, has shown, AREG has multiple and sometimes conflicting functions. This is reflected in the name amphi-regulin, whereby amphi means ´from both sides´ [158]. The question remains, why the same molecule can have these different functions, and how this is mediated.

One aspect to consider is post-translational protein modifications, which could influence AREG´s activities [159]. It is also possible that various, as yet unknown,

co-regulators like e.g. other EGFR ligands or pleiotropic cytokines may be expressed together with AREG and modulate its behavior. Furthermore, AREG's existence in soluble or membrane-bound forms adds another layer of complexity [160]. It is thus possible, that the membrane-bound form leads to different activation of the EGFR than soluble AREG and consequently induces pro- or anti-inflammatory signaling cascades.

The local AREG concentration also seems to be a critical factor influencing its biological effects. Studies in fibroblasts provide valuable insights into the dynamic nature of AREG-induced signaling pathways. In particular, the frequency of EGFR-induced oscillation of extracellular signal-regulated kinase (ERK) directly correlates with the strength of the induced proliferation signal. Albeck et al. have shown that higher ligand concentrations result in a higher pulse frequency, thereby enhancing the proliferation response [161].

However, the intricacies of AREG-induced signaling go beyond concentration-dependent effects. Low-affinity binding by AREG differs from the oscillatory signal observed with high-affinity EGFR ligands. Instead, sustained, and stable activation of ERK by low-affinity binding does not induce growth but rather leads to growth arrest and cell differentiation. This highlights the nuanced effects of AREG signaling duration on cellular biology [162]–[165].

Moreover, the differing biological processes that are induced by AREG signaling might be a result of AREG´s interactions with different cell types, each responding uniquely to the signal.

In addition, factors such as the unique migratory behavior of AREG-secreting cells, including differential niche trafficking to reach a defined subset of AREG-responsive cells, could underlie some of AREG´s differential functions.

It is also possible that the EGFR forms unique heterodimers with other receptor chains, as has recently been described [166], [167], which might result in differential effects.

Signaling through the EGFR may also be modified by intracellular adaptor proteins or their phosphorylation, glycosylation, lipidation, or ubiquitinylation, which differs from cell to cell and thus results in differential responses. Finally, it is also known, that small changes in the duration or even the strength of ligand binding to its receptor can lead to different responses in mitogen-activated protein kinase signaling associated with EGFR signaling [168]. Deciphering which of these mechanisms

influence AREG´s potent pro- and anti-inflammatory, as well as tissue reparative effects, will be crucial to developing AREG-directed therapies.

4.11. Therapeutic strategies

Experimental data by us and from many independent groups clearly suggest that non-specific, generalized administration or blockade of AREG is not the right treatment approach. Rather, a specific application reaching defined tissues or a cell type-specific neutralization of AREG or AREG signaling is required to achieve the desired therapeutic effects. My in vitro data nicely demonstrate that local administration of AREG could potentially be used to accelerate wound closure e.g. of injured skin and promote vascularization. However, it should be noted that excessive administration or administration at the wrong time point could conversely lead to fibrosis.

Considering my data from this thesis, it would also be conceivable to isolate Tregs from patients with LN, expand and stimulate them in vitro to produce AREG, and then give them back to the patient. Along this line, there are already studies showing that genetically modified human Tregs can be stimulated with IL-33 to produce AREG, which then polarizes macrophages towards the anti-inflammatory M2 subtype [169].

Another possibility would be to activate Macrophages and induce an M1 phenotype by AREG in acute bacterial inflammation via facilitation of AREG phagocytosis. The methods to precisely deliver drug molecules to specific cell types, particularly macrophages, have been substantially improved. Several studies have focused on using pattern recognition receptors on the surface of macrophages [170]. These receptors play a critical role in phagocytic clearance and can serve as targets for drug delivery. Success with receptors, as for example the lipoprotein receptor, underscores the possibility of developing targeted interventions based on receptor-specific interactions [171].

Another potential therapeutic strategy to target specific cells is bispecific antibodies. Bispecific antibodies represent an innovative approach in immunotherapy, designed to simultaneously engage two distinct targets [172]. In this approach, it is possible to design antibodies in which, one arm of the bispecific antibody is tailored to target CD4 cells by specifically recognizing surface structures associated with these immune cells. Upon binding to CD4 cells, the other arm of the antibody is engineered

to release AREG locally. This localized release of AREG would then modulate T-cell responses and downregulate their pro-inflammatory properties [126].

While there is still a great need for research to understand the intricate mechanisms and consequences of AREG/EGFR signaling, my work has revealed new insights and further supports the development of AREG-centered interventions as future therapeutic strategies.

5. Annex

5.1. Abbreviation

Table 6-1: List of abbreviations used in this study

Abbreviation	
%	Percent
°C	Degree Celcius
ANCA	Anti-neutrophil cytoplasmatic antibody
Ang II	Angiotensin II
AREG	Amphiregulin
BC	Bowman's capsule
C3	Complement component 3
CTLA-4	Cytotoxic T lymphocyte antigen 4
DC	Dendritic cells
DNA	Desoxy-ribucleic-acid
ECM	Extracellular matrix
EDTA	Ethylenediaminetetraacetic acid
EGF	Epidermal growth factor
EGFR	Epidermal growth factor receptor
ESKD	End-stage kidney disease
FACS	Fluorescence Activated Cell Sorting
FoxP3	Factor forkhead box P3
FSC	Forward scatter
g	Gram(s), earth acceleration
GBM	Glomerular basement membrane
glm	glomerular
GN	Glomerulonephritis
h	Hours
HB-EGF	Heparin-binding EGF-like growth factor
HBSS	Hanks' Balanced Salt Solution
hGEnC	Human glomerular endothelial cells
hpf	igh power field
IFNγ	Interferon gamma
IgG	Immunoglobuline G
IL	Interleukin
ILC-2	Innate lymphoid cell type 2
int	interstitial
LN	Lupus nephritis
LPS	Lipopolysaccharide
Ly6C	Lymphocyte antigen 6 complex, locus 6

M/M	Monocytes/macrophages
M1	Pro-inflammatory macrophages
M2	Anti-inflammatory macrophages
mg	Milligram(s)
min	Minutes
mL	Milliliter(s)
mMC	Murine Mesangial cells
MMP	Matrix metalloproteinases
mPTC	Proximal murine tubule cells
mTC	Murine tubular cells
NP-40	Nonident P40
OD	Optical density
PCR	Polymerase chain reaction
PD-1	Programmed cell death 1
PFA	Paraformaldehyde
PMA	Phorbol-12-myristate-13-acetate
pristane	2,6,10,14- tetramethylpentadecane
RNA	Ribonucleic acid
RPGN	Rapidly progressive GN
RT	Room-temperature
s	Seconds
SLE	Systemic Lupus erythematosus
SSC	Side scatter
TCR	T-cell-receptor
Teff	Effector T cells
TfH	T follicular helper cells
TGF-α	Transforming growth factor α
TGFβ	Transforming growth factor beta
Th1	T helper cell 1
Th17	T helper cell 17
Th2	T helper cell 2
TLR	Toll-like receptor
TNFα	Tumor necrosis factor alpha
Treg	Regulatory T cells
U	Units
UOO	Unilateral ureteral obstruction
µg	Microgram(s)
µL	Microliter(s)
µm	Mikrometer(s)

6. References

[1] B. Kaissling and M. Le Hir, "Characterization and distribution of interstitial cell types in the renal cortex of rats," *Kidney Int.*, vol. 45, no. 3, pp. 709–720, 1994.

[2] C. Kurts, U. Panzer, H. J. Anders, and A. J. Rees, "The immune system and kidney disease: Basic concepts and clinical implications," *Nat. Rev. Immunol.*, vol. 13, no. 10, pp. 738–753, 2013.

[3] A. Al Mushafi, J. D. Ooi, and D. Odobasic, "Crescentic Glomerulonephritis: Pathogenesis and Therapeutic Potential of Human Amniotic Stem Cells," *Front. Physiol.*, vol. 12, no. October, pp. 1–13, 2021.

[4] Arastéh K, *Innere Medizin*. Stuttgart: Thieme, 2018.

[5] A. Linke, G. Tiegs, and K. Neumann, "Pathogenic T-Cell Responses in Immune-Mediated Glomerulonephritis," *Cells*, vol. 11, no. 10, p. 1625, May 2022.

[6] W. G. Couser, "Glomerulonephritis," *Lancet*, vol. 353, no. 9163, pp. 1509–1515, May 1999.

[7] B. Smeets *et al.*, "Tracing the origin of glomerular extracapillary lesions from parietal epithelial cells," *J. Am. Soc. Nephrol.*, vol. 20, no. 12, pp. 2604–2615, 2009.

[8] D. B. G. O. C S Vinen, "Acute glomerulonephritis," *Postgr. Med Journa*, vol. 79, pp. 206–2013, 2003.

[9] S. Singh and R. Saxena, "Lupus nephritis," *Am. J. Med. Sci.*, vol. 337, no. 6, pp. 451–460, 2009.

[10] G. J. Pons-Estel, R. Serrano, M. A. Plasín, G. Espinosa, and R. Cervera, "Epidemiology and management of refractory lupus nephritis," *Autoimmun. Rev.*, vol. 10, no. 11, pp. 655–663, 2011.

[11] R. Cervera *et al.*, "Morbidity and mortality in systemic lupus erythematosus during a 10-year period: A comparison of early and late manifestations in a cohort of 1,000 patients," *Medicine (Baltimore).*, vol. 82, no. 5, pp. 299–308, 2003.

[12] S. C. Croca, T. Rodrigues, and D. A. Isenberg, "Assessment of a lupus nephritis cohort over a 30-year period.," *Rheumatology (Oxford).*, vol. 50, no. 8, pp. 1424–1430, 2011.

[13] S. Bernatsky *et al.*, "Mortality in systemic lupus erythematosus," *Arthritis Rheum.*, vol. 54, no. 8, pp. 2550–2557, 2006.

[14] F. A. Houssiau *et al.*, "Early response to immunosuppressive therapy predicts good renal outcome in lupus nephritis: Lessons from long-term followup of patients in the

euro-lupus nephritis trial," *Arthritis Rheum.*, vol. 50, no. 12, pp. 3934–3940, 2004.

[15] F. A. Houssiau and E. M. Ginzler, "Current treatment of lupus nephritis," *Lupus*, vol. 17, no. 5 SPEC. ISS., pp. 426–430, 2008.

[16] F. Tamirou and F. A. Houssiau, "Management of Lupus Nephritis," *J. Clin. Med.*, vol. 10, no. 4, p. 670, Feb. 2021.

[17] R. Banchereau *et al.*, "Personalized Immunomonitoring Uncovers Molecular Networks that Stratify Lupus Patients," *Cell*, vol. 165, no. 3, pp. 551–565, Apr. 2016.

[18] L. A. C. Rosen, G. Anhah, and A. Rosen, "Autoantigens targeted in systemic lupus erythematmus are clustered in two populations of surface structures on apoptotic keratinocytes," *J. Exp. Med.*, vol. 179, no. 4, pp. 1317–1330, 1994.

[19] U. S. Gaipl *et al.*, "Clearance deficiency and systemic lupus erythematosus (SLE)," *J. Autoimmun.*, vol. 28, no. 2–3, pp. 114–121, 2007.

[20] M. Herrmann, R. E. Voll, O. M. Zoller, M. Hagenhofer, B. B. Ponner, and J. R. Kalden, "Impaired phagocytosis of apoptotic cell material by monocyte-derived macrophages from patients with systemic lupus erythematosus," *Arthritis Rheum.*, vol. 41, no. 7, pp. 1241–1250, 1998.

[21] A. Ho, S. G. Barr, L. S. Magder, and M. Petri, "A decrease in complement is associated with increased renal and hematologic activity in patients with systemic lupus erythematosus," *Arthritis Rheum.*, vol. 44, no. 10, pp. 2350–2357, 2001.

[22] I. J. Gandino, M. Scolnik, E. Bertiller, V. Scaglioni, L. J. Catoggio, and E. R. Soriano, "Complement levels and risk of organ involvement in patients with systemic lupus erythematosus," *Lupus Sci. Med.*, vol. 4, no. 1, pp. 1–5, 2017.

[23] A. J. Swaak, J. Groenwold, and W. Bronsveld, "Predictive value of complement profiles and anti-dsDNA in systemic lupus erythematosus.," *Ann. Rheum. Dis.*, vol. 45, no. 5, pp. 359–366, May 1986.

[24] G. Sturfelt and L. Truedsson, "Complement and its breakdown products in SLE," *Rheumatology*, vol. 44, no. 10, pp. 1227–1232, Oct. 2005.

[25] G. Senaldi, V. A. Makinde, D. Vergani, and D. A. Isenberg, "Correlation of the activation of the fourth component of complement (C4) with disease activity in systemic lupus erythematosus.," *Ann. Rheum. Dis.*, vol. 47, no. 11, pp. 913–917, Nov. 1988.

[26] H.-J. Anders, R. Saxena, M. Zhao, I. Parodis, J. E. Salmon, and C. Mohan, "Lupus nephritis," *Nat. Rev. Dis. Prim.*, vol. 6, no. 1, p. 7, Jan. 2020.

[27] N. Rother and J. van der Vlag, "Disturbed T Cell Signaling and Altered Th17 and

Regulatory T Cell Subsets in the Pathogenesis of Systemic Lupus Erythematosus," *Front. Immunol.*, vol. 6, Nov. 2015.

[28] S. J. Kim, K. Lee, and B. Diamond, "Follicular Helper T Cells in Systemic Lupus Erythematosus," *Front. Immunol.*, vol. 9, Aug. 2018.

[29] K. Murphy, P. Travers, and M. Walport, *Janeway Immunologie*. Heidelberg: Spektrum Akademischer Verlag, 2009.

[30] D. Abdirama *et al.*, "Nuclear antigen–reactive CD4+ T cells expand in active systemic lupus erythematosus, produce effector cytokines, and invade the kidneys," *Kidney Int.*, vol. 99, no. 1, pp. 238–246, Jan. 2021.

[31] M. H. Foster, "T cells and B cells in lupus nephritis.," *Semin. Nephrol.*, vol. 27, no. 1, pp. 47–58, Jan. 2007.

[32] S.-C. Choi *et al.*, "Relative Contributions of B Cells and Dendritic Cells from Lupus-Prone Mice to CD4+ T Cell Polarization," *J. Immunol.*, vol. 200, no. 9, pp. 3087–3099, May 2018.

[33] H. Zhu *et al.*, "CD16+ Monocyte Subset Was Enriched and Functionally Exacerbated in Driving T-Cell Activation and B-Cell Response in Systemic Lupus Erythematosus," *Front. Immunol.*, vol. 7, Nov. 2016.

[34] G. M. Coppock *et al.*, "Loss of IL-27Rα Results in Enhanced Tubulointerstitial Fibrosis Associated with Elevated Th17 Responses," *J. Immunol.*, vol. 205, no. 2, pp. 377–386, Jul. 2020.

[35] C.-H. Weng *et al.*, "Interleukin-17A induces renal fibrosis through the ERK and Smad signaling pathways," *Biomed. Pharmacother.*, vol. 123, p. 109741, Mar. 2020.

[36] G. Amarilyo, E. V. Lourenço, F.-D. Shi, and A. La Cava, "IL-17 Promotes Murine Lupus," *J. Immunol.*, vol. 193, no. 2, pp. 540–543, Jul. 2014.

[37] S. A. Summers *et al.*, "Endogenous interleukin (IL)-17A promotes pristane-induced systemic autoimmunity and lupus nephritis induced by pristane," *Clin. Exp. Immunol.*, vol. 176, no. 3, pp. 341–350, Apr. 2014.

[38] O. M. Steinmetz *et al.*, "CXCR3 Mediates Renal Th1 and Th17 Immune Response in Murine Lupus Nephritis," *J. Immunol.*, vol. 183, no. 7, pp. 4693–4704, Oct. 2009.

[39] M. Yamada *et al.*, "Selective accumulation of CCR4+ T lymphocytes into renal tissue of patients with lupus nephritis," *Arthritis Rheum.*, vol. 46, no. 3, pp. 735–740, Mar. 2002.

[40] N. Charles, D. Hardwick, E. Daugas, G. G. Illei, and J. Rivera, "Basophils and the T helper 2 environment can promote the development of lupus nephritis," *Nat. Med.*,

vol. 16, no. 6, pp. 701–707, Jun. 2010.

[41] M. Gliwiński, D. Iwaszkiewicz-Grześ, and P. Trzonkowski, "Cell-Based Therapies with T Regulatory Cells," *BioDrugs*, vol. 31, no. 4, pp. 335–347, Aug. 2017.

[42] N. Mikami, R. Kawakami, and S. Sakaguchi, "New Treg cell-based therapies of autoimmune diseases: towards antigen-specific immune suppression," *Curr. Opin. Immunol.*, vol. 67, pp. 36–41, Dec. 2020.

[43] C. Mattozzi *et al.*, "Importance of Regulatory T Cells in the Pathogenesis of Psoriasis: Review of the Literature," *Dermatology*, vol. 227, no. 2, pp. 134–145, 2013.

[44] W. Y. Yang, Y. Shao, J. Lopez-Pastrana, J. Mai, H. Wang, and X. Yang, "Pathological conditions re-shape physiological Tregs into pathological Tregs," *Burn. Trauma*, vol. 3, Dec. 2015.

[45] M. Vaeth *et al.*, "Tissue resident and follicular Treg cell differentiation is regulated by CRAC channels," *Nat. Commun.*, vol. 10, no. 1, p. 1183, Mar. 2019.

[46] K. N. Couper, D. G. Blount, and E. M. Riley, "IL-10: The Master Regulator of Immunity to Infection," *J. Immunol.*, vol. 180, no. 9, pp. 5771–5777, May 2008.

[47] Y. Y. Wan and R. A. Flavell, "'Yin–Yang' functions of transforming growth factor-β and T regulatory cells in immune regulation," *Immunol. Rev.*, vol. 220, no. 1, pp. 199–213, Dec. 2007.

[48] V. Chaturvedi, L. W. Collison, C. S. Guy, C. J. Workman, and D. A. A. Vignali, "Cutting Edge: Human Regulatory T Cells Require IL-35 To Mediate Suppression and Infectious Tolerance," *J. Immunol.*, vol. 186, no. 12, pp. 6661–6666, Jun. 2011.

[49] M. Yadav *et al.*, "Neuropilin-1 distinguishes natural and inducible regulatory T cells among regulatory T cell subsets in vivo," *J. Exp. Med.*, vol. 209, no. 10, pp. 1713–1722, Sep. 2012.

[50] R. A. Peterson, "Regulatory T-Cells: Diverse Phenotypes Integral to Immune Homeostasis and Suppression," *Toxicol. Pathol.*, vol. 40, no. 2, pp. 186–204, Feb. 2012.

[51] F. Bayati, M. Mohammadi, M. Valadi, S. Jamshidi, A. M. Foma, and E. Sharif-Paghaleh, "The Therapeutic Potential of Regulatory T Cells: Challenges and Opportunities," *Front. Immunol.*, vol. 11, Jan. 2021.

[52] W. J. Grossman, J. W. Verbsky, W. Barchet, M. Colonna, J. P. Atkinson, and T. J. Ley, "Human T Regulatory Cells Can Use the Perforin Pathway to Cause Autologous Target Cell Death," *Immunity*, vol. 21, no. 4, pp. 589–601, Oct. 2004.

[53] J. Loebbermann *et al.*, "Regulatory T cells expressing granzyme B play a critical role

in controlling lung inflammation during acute viral infection," *Mucosal Immunol.*, vol. 5, no. 2, pp. 161–172, Mar. 2012.

[54] G. Borsellino *et al.*, "Expression of ectonucleotidase CD39 by Foxp3+ Treg cells: hydrolysis of extracellular ATP and immune suppression," *Blood*, vol. 110, no. 4, pp. 1225–1232, Aug. 2007.

[55] G. R. Herrnstadt and O. M. Steinmetz, "The role of Treg subtypes in glomerulonephritis," *Cell Tissue Res.*, no. 0123456789, 2020.

[56] T. Hayashi, K. Hasegawa, and C. Adachi, "Elimination of CD4 + CD25 + T cell accelerates the development of glomerulonephritis during the preactive phase in autoimmune-prone female NZB × NZW F 1 mice," *Int. J. Exp. Pathol.*, vol. 86, no. 5, pp. 289–296, Oct. 2005.

[57] K. J. Scalapino, Q. Tang, J. A. Bluestone, M. L. Bonyhadi, and D. I. Daikh, "Suppression of Disease in New Zealand Black/New Zealand White Lupus-Prone Mice by Adoptive Transfer of Ex Vivo Expanded Regulatory T Cells," *J. Immunol.*, vol. 177, no. 3, pp. 1451–1459, Aug. 2006.

[58] M. A. Kluger *et al.*, "Treg17 cells are programmed by Stat3 to suppress Th17 responses in systemic lupus," *Kidney Int.*, vol. 89, no. 1, pp. 158–166, Jan. 2016.

[59] M. A. Kluger *et al.*, "Rorγt expression in Tregspromotes systemic lupus erythematosus VIA IL-17 secretion, alteration of Tregphenotype and suppression of Th2 responses," *Clin. Exp. Immunol.*, vol. 188, no. 1, pp. 63–78, 2017.

[60] J. Nie, Y. Y. Li, S. G. Zheng, A. Tsun, and B. Li, "FOXP3+ Treg Cells and Gender Bias in Autoimmune Diseases," *Front. Immunol.*, vol. 6, Sep. 2015.

[61] M. Bonelli *et al.*, "Quantitative and qualitative deficiencies of regulatory T cells in patients with systemic lupus erythematosus (SLE)," *Int. Immunol.*, vol. 20, no. 7, pp. 861–868, Apr. 2008.

[62] M. Miyara *et al.*, "Global Natural Regulatory T Cell Depletion in Active Systemic Lupus Erythematosus," *J. Immunol.*, vol. 175, no. 12, pp. 8392–8400, Dec. 2005.

[63] K. Ohl and K. Tenbrock, "Regulatory T cells in systemic lupus erythematosus," *Eur. J. Immunol.*, vol. 45, no. 2, pp. 344–355, Feb. 2015.

[64] M. Mizui and G. C. Tsokos, "Targeting Regulatory T Cells to Treat Patients With Systemic Lupus Erythematosus," *Front. Immunol.*, vol. 9, Apr. 2018.

[65] Y. Zhu, Y. Huang, B. Ming, X. Wu, Y. Chen, and L. Dong, "Regulatory T-cell levels in systemic lupus erythematosus patients: a meta-analysis," *Lupus*, vol. 28, no. 4, pp. 445–454, Apr. 2019.

[66] J. He *et al.*, “Low-dose interleukin-2 treatment selectively modulates CD4+ T cell subsets in patients with systemic lupus erythematosus,” *Nat. Med.*, vol. 22, no. 9, pp. 991–993, Sep. 2016.

[67] A. Shapouri-Moghaddam *et al.*, “Macrophage plasticity, polarization, and function in health and disease,” *J. Cell. Physiol.*, vol. 233, no. 9, pp. 6425–6440, Sep. 2018.

[68] B. T. Fife, G. B. Huffnagle, W. A. Kuziel, and W. J. Karpus, “Cc Chemokine Receptor 2 Is Critical for Induction of Experimental Autoimmune Encephalomyelitis,” *J. Exp. Med.*, vol. 192, no. 6, pp. 899–906, Sep. 2000.

[69] E. Zigmond *et al.*, “Ly6Chi Monocytes in the Inflamed Colon Give Rise to Proinflammatory Effector Cells and Migratory Antigen-Presenting Cells,” *Immunity*, vol. 37, no. 6, pp. 1076–1090, Dec. 2012.

[70] S. C. Funes, M. Rios, J. Escobar-Vera, and A. M. Kalergis, “Implications of macrophage polarization in autoimmunity,” *Immunology*, vol. 154, no. 2, pp. 186–195, Jun. 2018.

[71] S. Gordon and P. R. Taylor, “Monocyte and macrophage heterogeneity,” *Nat. Rev. Immunol.*, vol. 5, no. 12, pp. 953–964, Dec. 2005.

[72] N. Wang, H. Liang, and K. Zen, “Molecular Mechanisms That Influence the Macrophage M1â€“M2 Polarization Balance,” *Front. Immunol.*, vol. 5, Nov. 2014.

[73] S. R. Holdsworth and P. G. Tipping, “Leukocytes in glomerular injury,” *Semin. Immunopathol.*, vol. 29, no. 4, pp. 355–374, Oct. 2007.

[74] M. A. Kluger *et al.*, “Leukocyte-derived MMP9 is crucial for the recruitment of proinflammatory macrophages in experimental glomerulonephritis,” *Kidney Int.*, vol. 83, no. 5, pp. 865–877, May 2013.

[75] M. Luig *et al.*, “Inflammation-Induced IL-6 Functions as a Natural Brake on Macrophages and Limits GN,” *J. Am. Soc. Nephrol.*, vol. 26, no. 7, pp. 1597–1607, Jul. 2015.

[76] A. Arazi *et al.*, “The immune cell landscape in kidneys of patients with lupus nephritis,” *Nat. Immunol.*, vol. 20, no. 7, pp. 902–914, Jul. 2019.

[77] Y. Cao, W. Tang, and W. Tang, “Immune cell infiltration characteristics and related core genes in lupus nephritis: results from bioinformatic analysis,” *BMC Immunol.*, vol. 20, no. 1, p. 37, Dec. 2019.

[78] K. S. Peterson *et al.*, “Characterization of heterogeneity in the molecular pathogenesis of lupus nephritis from transcriptional profiles of laser-captured glomeruli,” *J. Clin. Invest.*, vol. 113, no. 12, pp. 1722–1733, Jun. 2004.

[79] L. E. Kwant *et al.*, "Macrophages in Lupus Nephritis: Exploring a potential new therapeutic avenue," *Autoimmun. Rev.*, vol. 21, no. 12, p. 103211, Dec. 2022.

[80] W. Zhang *et al.*, "DNA-dependent Activator of Interferon-regulatory Factors (DAI) Promotes Lupus Nephritis by Activating the Calcium Pathway," *J. Biol. Chem.*, vol. 288, no. 19, pp. 13534–13550, May 2013.

[81] X. Chen, Z. Wen, W. Xu, and S. Xiong, "Granulin Exacerbates Lupus Nephritis via Enhancing Macrophage M2b Polarization," *PLoS One*, vol. 8, no. 6, p. e65542, Jun. 2013.

[82] W. Zhang, W. Xu, and S. Xiong, "Macrophage Differentiation and Polarization via Phosphatidylinositol 3-Kinase/Akt–ERK Signaling Pathway Conferred by Serum Amyloid P Component," *J. Immunol.*, vol. 187, no. 4, pp. 1764–1777, Aug. 2011.

[83] Y. Cai, W. Zhang, and S. Xiong, "Mannose-Binding Lectin Blunts Macrophage Polarization and Ameliorates Lupus Nephritis," *PLoS One*, vol. 8, no. 4, p. e62465, Apr. 2013.

[84] F. Li, Y. Yang, X. Zhu, L. Huang, and J. Xu, "Macrophage Polarization Modulates Development of Systemic Lupus Erythematosus," *Cell. Physiol. Biochem.*, vol. 37, no. 4, pp. 1279–1288, 2015.

[85] Z. Zhang *et al.*, "Mesenchymal stem cells prevent podocyte injury in lupus-prone B6.MRL- Faslpr mice via polarizing macrophage into an anti-inflammatory phenotype," *Nephrol. Dial. Transplant.*, vol. 34, no. 4, pp. 597–605, Apr. 2019.

[86] B. Horuluoglu, D. Bayik, N. Kayraklioglu, E. Goguet, M. J. Kaplan, and D. M. Klinman, "PAM3 supports the generation of M2-like macrophages from lupus patient monocytes and improves disease outcome in murine lupus," *J. Autoimmun.*, vol. 99, pp. 24–32, May 2019.

[87] D. C. Rockey, P. D. Bell, and J. A. Hill, "Fibrosis — A Common Pathway to Organ Injury and Failure," *N. Engl. J. Med.*, vol. 372, no. 12, pp. 1138–1149, 2015.

[88] T. Wynn, "Cellular and molecular mechanisms of fibrosis," *J. Pathol.*, vol. 214, no. 2, pp. 199–210, Jan. 2008.

[89] T. A. Wynn, "Common and unique mechanisms regulate fibrosis in various fibroproliferative diseases," *J. Clin. Invest.*, vol. 117, no. 3, pp. 524–529, 2007.

[90] J. H. W. Distler, A.-H. Györfi, M. Ramanujam, M. L. Whitfield, M. Königshoff, and R. Lafyatis, "Shared and distinct mechanisms of fibrosis," *Nat. Rev. Rheumatol.*, vol. 15, no. 12, pp. 705–730, Dec. 2019.

[91] S. Sciascia *et al.*, "Renal Fibrosis in Lupus Nephritis," *Int. J. Mol. Sci.*, vol. 23, no.

22, p. 14317, Nov. 2022.

[92] A. Pardo and M. Selman, “Matrix metalloproteases in aberrant fibrotic tissue remodeling,” *Proc. Am. Thorac. Soc.*, vol. 3, no. 4, pp. 383–388, 2006.

[93] P. M. K. Tang, D. J. Nikolic-Paterson, and H. Y. Lan, “Macrophages: versatile players in renal inflammation and fibrosis,” *Nat. Rev. Nephrol.*, vol. 15, no. 3, pp. 144–158, 2019.

[94] D. J. Nikolic-Paterson, S. Wang, and H. Y. Lan, “Macrophages promote renal fibrosis through direct and indirect mechanisms,” *Kidney Int. Suppl.*, vol. 4, no. 1, pp. 34–38, 2014.

[95] M. G. Kim, S. C. Kim, Y. S. Ko, H. Y. Lee, S. K. Jo, and W. Cho, “The role of M2 macrophages in the progression of chronic kidney disease following acute kidney injury,” *PLoS One*, vol. 10, no. 12, pp. 1–17, 2015.

[96] P. Romagnani *et al.*, “Chronic kidney disease,” *Nat. Rev. Dis. Prim.*, vol. 3, 2017.

[97] Y. Liu, “Renal fibrosis: New insights into the pathogenesis and therapeutics,” *Kidney Int.*, vol. 69, no. 2, pp. 213–217, 2006.

[98] P. Boor and J. Floege, “Renal allograft fibrosis: Biology and therapeutic targets,” *Am. J. Transplant.*, vol. 15, no. 4, pp. 863–886, 2015.

[99] J. A. Krall, E. M. Beyer, and G. MacBeath, “High- and Low-Affinity Epidermal Growth Factor Receptor-Ligand Interactions Activate Distinct Signaling Pathways,” *PLoS One*, vol. 6, no. 1, p. e15945, Jan. 2011.

[100] D. M. Zaiss, C. M. Minutti, and J. A. Knipper, “Immune- and non-immune-mediated roles of regulatory T-cells during wound healing,” *Immunology*, vol. 157, no. 3, pp. 190–197, 2019.

[101] E. Kefaloyianni *et al.*, “ADAM17 substrate release in proximal tubule drives kidney fibrosis,” *JCI Insight*, vol. 1, no. 13, Aug. 2016.

[102] Y. Yarden and M. X. Sliwkowski, “Untangling the ErbB signalling network,” *Nat. Rev. Mol. Cell Biol.*, vol. 2, no. 2, pp. 127–137, Feb. 2001.

[103] J. Tang, N. Liu, and S. Zhuang, “Role of epidermal growth factor receptor in acute and chronic kidney injury,” *Kidney Int.*, vol. 83, no. 5, pp. 804–810, May 2013.

[104] W. B. W. H. Melenhorst *et al.*, “Epidermal Growth Factor Receptor Signaling in the Kidney,” *Hypertension*, vol. 52, no. 6, pp. 987–993, Dec. 2008.

[105] H. D. Humes, D. A. Cieslinski, T. M. Coimbra, J. M. Messana, and C. Galvao, “Epidermal growth factor enhances renal tubule cell regeneration and repair and accelerates the recovery of renal function in postischemic acute renal failure.,” *J. Clin.*

Invest., vol. 84, no. 6, pp. 1757–1761, Dec. 1989.

[106] Z. Wang, J.-K. Chen, S. Wang, G. Moeckel, and R. C. Harris, "Importance of Functional EGF Receptors in Recovery from Acute Nephrotoxic Injury," *J. Am. Soc. Nephrol.*, vol. 14, no. 12, pp. 3147–3154, Dec. 2003.

[107] N. Liu *et al.*, "Genetic or Pharmacologic Blockade of EGFR Inhibits Renal Fibrosis," *J. Am. Soc. Nephrol.*, vol. 23, no. 5, pp. 854–867, May 2012.

[108] L. Wassef, D. J. Kelly, and R. E. Gilbert, "Epidermal growth factor receptor inhibition attenuates early kidney enlargement in experimental diabetes," *Kidney Int.*, vol. 66, no. 5, pp. 1805–1814, Nov. 2004.

[109] H. François *et al.*, "Prevention of renal vascular and glomerular fibrosis by epidermal growth factor receptor inhibition," *FASEB J.*, vol. 18, no. 7, pp. 926–928, May 2004.

[110] J. Chen, J.-K. Chen, and R. C. Harris, "Deletion of the epidermal growth factor receptor in renal proximal tubule epithelial cells delays recovery from acute kidney injury," *Kidney Int.*, vol. 82, no. 1, pp. 45–52, Jul. 2012.

[111] W. G. Richards, W. E. Sweeney, B. K. Yoder, J. E. Wilkinson, R. P. Woychik, and E. D. Avner, "Epidermal growth factor receptor activity mediates renal cyst formation in polycystic kidney disease.," *J. Clin. Invest.*, vol. 101, no. 5, pp. 935–939, Mar. 1998.

[112] G. Bollée *et al.*, "Epidermal growth factor receptor promotes glomerular injury and renal failure in rapidly progressive crescentic glomerulonephritis," *Nat. Med.*, vol. 17, no. 10, pp. 1242–1250, Oct. 2011.

[113] S. Zhuang and N. Liu, "EGFR signaling in renal fibrosis," *Kidney Int. Suppl.*, vol. 4, no. 1, pp. 70–74, Nov. 2014.

[114] X. Qing *et al.*, "iRhom2 promotes lupus nephritis through TNF-α and EGFR signaling," *J. Clin. Invest.*, vol. 128, no. 4, pp. 1397–1412, Apr. 2018.

[115] J. Liu *et al.*, "GPR174 knockdown enhances blood fl ow recovery in hindlimb ischemia mice model by upregulating AREG expression," 2022.

[116] C. M. Minutti *et al.*, "A Macrophage-Pericyte Axis Directs Tissue Restoration via Amphiregulin-Induced Transforming Growth Factor Beta Activation," *Immunity*, vol. 50, no. 3, pp. 645-654.e6, 2019.

[117] K. Fujiu *et al.*, "A heart–brain–kidney network controls adaptation to cardiac stress through tissue macrophage activation," *Nat. Med.*, vol. 23, no. 5, pp. 611–622, May 2017.

[118] J. H. Ko, H. J. Kim, H. J. Jeong, H. J. Lee, and J. Y. Oh, "Mesenchymal Stem and

Stromal Cells Harness Macrophage-Derived Amphiregulin to Maintain Tissue Homeostasis," *Cell Rep.*, vol. 30, no. 11, pp. 3806-3820.e6, Mar. 2020.

[119] D. Burzyn *et al.*, "A Special Population of Regulatory T Cells Potentiates Muscle Repair," *Cell*, vol. 155, no. 6, pp. 1282–1295, Dec. 2013.

[120] L. A. Monticelli, L. C. Osborne, M. Noti, S. V. Tran, D. M. W. Zaiss, and D. Artis, "IL-33 promotes an innate immune pathway of intestinal tissue protection dependent on amphiregulin-EGFR interactions," *Proc. Natl. Acad. Sci. U. S. A.*, vol. 112, no. 34, pp. 10762–10767, 2015.

[121] L. A. Monticelli *et al.*, "Innate lymphoid cells promote lung-tissue homeostasis after infection with influenza virus.," *Nat. Immunol.*, vol. 12, no. 11, pp. 1045–54, Nov. 2011.

[122] Q. Cao *et al.*, "Potentiating Tissue-Resident Type 2 Innate Lymphoid Cells by IL-33 to Prevent Renal Ischemia-Reperfusion Injury," *J. Am. Soc. Nephrol.*, vol. 29, no. 3, pp. 961–976, Mar. 2018.

[123] C. M. Minutti *et al.*, "Epidermal Growth Factor Receptor Expression Licenses Type-2 Helper T Cells to Function in a T Cell Receptor-Independent Fashion," *Immunity*, vol. 47, no. 4, pp. 710-722.e6, Oct. 2017.

[124] D. M. W. Zaiss *et al.*, "Amphiregulin Enhances Regulatory T Cell-Suppressive Function via the Epidermal Growth Factor Receptor," *Immunity*, vol. 38, no. 2, pp. 275–284, Feb. 2013.

[125] Y. Qi *et al.*, "Human basophils express amphiregulin in response to T cell–derived IL-3," *J. Allergy Clin. Immunol.*, vol. 126, no. 6, pp. 1260-1266.e4, Dec. 2010.

[126] S. Melderis *et al.*, "The Amphiregulin/EGFR axis protects from lupus nephritis via downregulation of pathogenic CD4+ T helper cell responses," *J. Autoimmun.*, vol. 129, p. 102829, May 2022.

[127] P. W. Cook *et al.*, "Transgenic expression of the human amphiregulin gene induces a psoriasis-like phenotype.," *J. Clin. Invest.*, vol. 100, no. 9, pp. 2286–2294, Nov. 1997.

[128] Y. Morimoto *et al.*, "Amphiregulin-Producing Pathogenic Memory T Helper 2 Cells Instruct Eosinophils to Secrete Osteopontin and Facilitate Airway Fibrosis," *Immunity*, vol. 49, no. 1, pp. 134-150.e6, Jul. 2018.

[129] S. Lisi *et al.*, "Pro-inflammatory role of Anti-Ro/SSA autoantibodies through the activation of Furin–TACE–amphiregulin axis," *J. Autoimmun.*, vol. 35, no. 2, pp. 160–170, Sep. 2010.

[130] S. Yamane *et al.*, "Proinflammatory role of amphiregulin, an epidermal growth factor

family member whose expression is augmented in rheumatoid arthritis patients," *J. Inflamm.*, vol. 5, no. 1, p. 5, 2008.

[131] S. Melderis *et al.*, "Amphiregulin Aggravates Glomerulonephritis via Recruitment and Activation of Myeloid Cells," *J. Am. Soc. Nephrol.*, vol. 31, no. 9, pp. 1996–2012, 2020.

[132] A. Lautrette *et al.*, "Angiotensin II and EGF receptor cross-talk in chronic kidney diseases: a new therapeutic approach," *Nat. Med.*, vol. 11, no. 8, pp. 867–874, Aug. 2005.

[133] M. J. Perugorria *et al.*, "The epidermal growth factor receptor ligand amphiregulin participates in the development of mouse liver fibrosis," *Hepatology*, vol. 48, no. 4, pp. 1251–1261, Oct. 2008.

[134] W.-H. Cheng *et al.*, "Amphiregulin induces CCN2 and fibronectin expression by TGF-β through EGFR-dependent pathway in lung epithelial cells," *Respir. Res.*, vol. 23, no. 1, p. 381, Dec. 2022.

[135] M. Y. Zhang *et al.*, "A critical role of AREG for bleomycin-induced skin fibrosis," *Cell Biosci.*, vol. 11, no. 1, p. 40, Dec. 2021.

[136] Y. Zhou *et al.*, "Amphiregulin, an Epidermal Growth Factor Receptor Ligand, Plays an Essential Role in the Pathogenesis of Transforming Growth Factor-β-induced Pulmonary Fibrosis," *J. Biol. Chem.*, vol. 287, no. 50, pp. 41991–42000, Dec. 2012.

[137] E. Kefaloyianni *et al.*, "Proximal tubule-derived amphiregulin amplifies and integrates profibrotic EGF receptor signals in kidney fibrosis," *J. Am. Soc. Nephrol.*, vol. 30, no. 12, pp. 2370–2383, 2019.

[138] S. C. Satchell *et al.*, "Conditionally immortalized human glomerular endothelial cells expressing fenestrations in response to VEGF," *Kidney Int.*, vol. 69, no. 9, pp. 1633–1640, May 2006.

[139] G. Wolf, E. Mueller, R. A. Stahl, and F. N. Ziyadeh, "Angiotensin II-induced hypertrophy of cultured murine proximal tubular cells is mediated by endogenous transforming growth factor-beta.," *J. Clin. Invest.*, vol. 92, no. 3, pp. 1366–1372, Sep. 1993.

[140] G. Wolf, U. Haberstroh, and E. G. Neilson, "Angiotensin II stimulates the proliferation and biosynthesis of type I collagen in cultured murine mesangial cells.," *Am. J. Pathol.*, vol. 140, no. 1, pp. 95–107, Jan. 1992.

[141] R. K. S. Phoon, A. R. Kitching, D. Odobasic, L. K. Jones, T. J. Semple, and S. R. Holdsworth, "T-bet Deficiency Attenuates Renal Injury in Experimental Crescentic

Glomerulonephritis," *J. Am. Soc. Nephrol.*, vol. 19, no. 3, pp. 477–485, Mar. 2008.

[142] F. Bonomini, M. Dos Santos, F. V. Veronese, and R. Rezzani, "NLRP3 Inflammasome Modulation by Melatonin Supplementation in Chronic Pristane-Induced Lupus Nephritis," *Int. J. Mol. Sci.*, vol. 20, no. 14, p. 3466, Jul. 2019.

[143] S. A. Summers *et al.*, "TLR9 and TLR4 are required for the development of autoimmunity and lupus nephritis in pristane nephropathy," *J. Autoimmun.*, vol. 35, no. 4, pp. 291–298, Dec. 2010.

[144] G. Carpentier *et al.*, "Angiogenesis Analyzer for ImageJ — A comparative morphometric analysis of 'Endothelial Tube Formation Assay' and 'Fibrin Bead Assay,'" *Sci. Rep.*, vol. 10, no. 1, p. 11568, Jul. 2020.

[145] D. M. W. Zaiss, W. C. Gause, L. C. Osborne, and D. Artis, "Emerging functions of amphiregulin in orchestrating immunity, inflammation, and tissue repair," *Immunity*, vol. 42, no. 2, pp. 216–226, 2015.

[146] S. Krishnan *et al.*, "Amphiregulin-producing γδ T cells are vital for safeguarding oral barrier immune homeostasis," *Proc. Natl. Acad. Sci.*, vol. 115, no. 42, pp. 10738–10743, Oct. 2018.

[147] C. Meulenbroeks *et al.*, "Basophil-Derived Amphiregulin Is Essential for UVB Irradiation–Induced Immune Suppression," *J. Invest. Dermatol.*, vol. 135, no. 1, pp. 222–228, Jan. 2015.

[148] M. D. Aupperlee *et al.*, "Epidermal Growth Factor Receptor (EGFR) Signaling Is a Key Mediator of Hormone-Induced Leukocyte Infiltration in the Pubertal Female Mammary Gland," *Endocrinology*, vol. 155, no. 6, pp. 2301–2313, Jun. 2014.

[149] H. Harb *et al.*, "Notch4 signaling limits regulatory T-cell-mediated tissue repair and promotes severe lung inflammation in viral infections," *Immunity*, vol. 54, no. 6, pp. 1186-1199.e7, Jun. 2021.

[150] Y. Ikeno *et al.*, "Foxp3+ Regulatory T Cells Inhibit CCl4-Induced Liver Inflammation and Fibrosis by Regulating Tissue Cellular Immunity," *Front. Immunol.*, vol. 11, Oct. 2020.

[151] B. Son *et al.*, "SAMiRNA Targeting Amphiregulin Alleviate Total-Body-Irradiation-Induced Renal Fibrosis," *Radiat. Res.*, vol. 197, no. 5, Feb. 2022.

[152] S. S. Son *et al.*, "In vivo silencing of amphiregulin by a novel effective Self-Assembled-Micelle inhibitory RNA ameliorates renal fibrosis via inhibition of EGFR signals," *Sci. Rep.*, vol. 11, no. 1, p. 2191, Jan. 2021.

[153] S. Cao *et al.*, "EGFR-mediated activation of adipose tissue macrophages promotes

obesity and insulin resistance," *Nat. Commun.*, vol. 13, no. 1, p. 4684, Aug. 2022.

[154] J. Sugita *et al.*, "Cardiac macrophages prevent sudden death during heart stress," *Nat. Commun.*, vol. 12, no. 1, p. 1910, Mar. 2021.

[155] N. Arpaia *et al.*, "A Distinct Function of Regulatory T Cells in Tissue Protection," *Cell*, vol. 162, no. 5, pp. 1078–1089, 2015.

[156] K. A. Kaiser, L. F. Loffredo, K. de los Santos-Alexis, O. R. Ringham, and N. Arpaia, "Regulation of the alveolar regenerative niche by amphiregulin-producing regulatory T cells," *J. Exp. Med.*, vol. 220, no. 3, Mar. 2023.

[157] X. Yu, A. Radulescu, C.-L. Chen, I. O. James, and G. E. Besner, "Heparin-Binding EGF-Like Growth Factor Protects Pericytes from Injury," *J. Surg. Res.*, vol. 172, no. 1, pp. 165–176, Jan. 2012.

[158] M. Shoyab, V. L. McDonald, J. G. Bradley, and G. J. Todaro, "Amphiregulin: a bifunctional growth-modulating glycoprotein produced by the phorbol 12-myristate 13-acetate-treated human breast adenocarcinoma cell line MCF-7.," *Proc. Natl. Acad. Sci.*, vol. 85, no. 17, pp. 6528–6532, Sep. 1988.

[159] S. Ramazi and J. Zahiri, "Post-translational modifications in proteins: resources, tools and prediction methods," *Database*, vol. 2021, Apr. 2021.

[160] V. Hosur, M. L. Farley, L. M. Burzenski, L. D. Shultz, and M. V. Wiles, "ADAM17 is essential for ectodomain shedding of the EGF-receptor ligand amphiregulin," *FEBS Open Bio*, vol. 8, no. 4, pp. 702–710, Apr. 2018.

[161] J. G. Albeck, G. B. Mills, and J. S. Brugge, "Frequency-Modulated Pulses of ERK Activity Transmit Quantitative Proliferation Signals," *Mol. Cell*, vol. 49, no. 2, pp. 249–261, Jan. 2013.

[162] I. Imayoshi *et al.*, "Oscillatory Control of Factors Determining Multipotency and Fate in Mouse Neural Progenitors," *Science (80-.).*, vol. 342, no. 6163, pp. 1203–1208, Dec. 2013.

[163] C. . Marshall, "Specificity of receptor tyrosine kinase signaling: Transient versus sustained extracellular signal-regulated kinase activation," *Cell*, vol. 80, no. 2, pp. 179–185, Jan. 1995.

[164] L. Pasic *et al.*, "Sustained activation of the HER1–ERK1/2–RSK signaling pathway controls myoepithelial cell fate in human mammary tissue," *Genes Dev.*, vol. 25, no. 15, pp. 1641–1653, Aug. 2011.

[165] S. Traverse, N. Gomez, H. Paterson, C. Marshall, and P. Cohen, "Sustained activation of the mitogen-activated protein (MAP) kinase cascade may be required for

differentiation of PC12 cells. Comparison of the effects of nerve growth factor and epidermal growth factor," *Biochem. J.*, vol. 288, no. 2, pp. 351–355, Dec. 1992.

[166] R. Goldman, R. Ben Levy, E. Peles, and Y. Yarden, "Heterodimerization of the erbB-1 and erbB-2 receptors in human breast carcinoma cells: a mechanism for receptor transregulation," *Biochemistry*, vol. 29, no. 50, pp. 11024–11028, Dec. 1990.

[167] X. Bai *et al.*, "Structure and dynamics of the EGFR/HER2 heterodimer," *Cell Discov.*, vol. 9, no. 1, p. 18, Feb. 2023.

[168] P. Andreu-Pérez *et al.*, "Protein Arginine Methyltransferase 5 Regulates ERK1/2 Signal Transduction Amplitude and Cell Fate Through CRAF," *Sci. Signal.*, vol. 4, no. 190, Sep. 2011.

[169] A. J. Lam *et al.*, "Innate Control of Tissue-Reparative Human Regulatory T Cells," *J. Immunol.*, vol. 202, no. 8, pp. 2195–2209, Apr. 2019.

[170] Z. Hong *et al.*, "Specifically targeted delivery of protein to phagocytic macrophages," *Int. J. Nanomedicine*, p. 1743, Mar. 2015.

[171] X. Gu *et al.*, "Preparation and Characterization of a Lovastatin-Loaded Protein-Free Nanostructured Lipid Carrier Resembling High-Density Lipoprotein and Evaluation of its Targeting to Foam Cells," *AAPS PharmSciTech*, vol. 12, no. 4, pp. 1200–1208, Dec. 2011.

[172] A. F. Labrijn, M. L. Janmaat, J. M. Reichert, and P. W. H. I. Parren, "Bispecific antibodies: a mechanistic review of the pipeline," *Nat. Rev. Drug Discov.*, vol. 18, no. 8, pp. 585–608, Aug. 2019.